Formability Analysis of Metal-Polymer Sandwich Composites Considering the Adhesion Strength

Tsegaye Bekele Tufa

A Thesis Submitted to

The department of Mechanical Design and Manufacturing Engineering

School of Mechanical, Chemical and Materials Engineering

Presented in Partial Fulfillment of the Requirement for the Degree of Master's in Manufacturing Engineering

Office of Graduate Studies

Adama Science and Technology University

February, 2022

Adama, Ethiopia

Formability Analysis of Metal-Polymer Sandwich Composites Considering the Adhesion Strength

Tsegaye Bekele Tufa

Advisor: Dr. Perumalla Janaki Ramulu

Co-Advisor: Dr. Habtamu B.

A Thesis Submitted to

The department of Mechanical Design and Manufacturing Engineering

School of Mechanical, Chemical and Materials Engineering

Presented in Partial Fulfillment of the Requirement for the Degree of Master’s in Manufacturing Engineering

Office of Graduate Studies

Adama Science and Technology University

February, 2022

Adama, Ethiopia

Declaration

I hereby declare that this Master Thesis entitled “Formability Analysis of Metal-Polymer Sandwich Composites Considering the Adhesion Strength” is my original work. That is, it has not been submitted for the award of any academic degree, diploma or certificate in any other university. All sources of materials that are used for this thesis have been duly acknowledged through citation.

Name of the student	Signature	Date

Approval Page of M.Sc. Thesis

I/we, the advisors of the thesis entitled "Formability Analysis of Metal-Polymer Sandwich Composites Considering the Adhesion Strength" and developed by Tsegaye Bekele, hereby certify that the recommendation and suggestions made by the board of examiners are appropriately incorporated into the final version of the thesis.

______________________	______________________	______________
Major Advisor	Signature	Date
______________________	______________________	______________
Co-advisor	Signature	Date

We, the undersigned, members of the Board of Examiners of the thesis by Tsegaye Bekele have read and evaluated the thesis entitled "Formability Analysis of Metal-Polymer Sandwich Composites Considering the Adhesion Strength" and examined the candidate during open defense. This is, therefore, to certify that the thesis is accepted for partial fulfillment of the requirement of the degree of Master of Science in Manufacturing Engineering.

______________________	______________________	______________
Chairperson	Signature	Date
______________________	______________________	______________
Internal Examiner	Signature	Date
______________________	______________________	______________
External Examiner	Signature	Date

Final approval and acceptance of the thesis is contingent upon submission of its final copy to the Office of Postgraduate Studies (OPGS) through the Department Graduate Council (DGC) and School Graduate Committee (SGC).

______________________	______________________	______________
Department Head	Signature	Date
______________________	______________________	______________
School Dean	Signature	Date
______________________	______________________	______________
Office of Postgraduate Studies, Dean	Signature	Date

Recommendation

I/we, the advisor(s) of this thesis, hereby certify that I/we have read the revised version of the thesis entitled "Formability Analysis of Metal-Polymer Sandwich Composites Considering the Adhesion Strength" prepared under my/our guidance by Tsegaye Bekele submitted in partial fulfillment of the requirements for the degree of Masters of Science in Manufacturing Engineering.

Therefore, I/we recommend the submission of revised version of the thesis to the department following the applicable procedures.

___________________________	________________________	________________
Major Advisor	Signature	Date
___________________________	________________________	________________
Co-advisor	Signature	Date

Acknowledgement

First of all, I would like to thank God Almighty for giving me the opportunity and guidance to achieving my goal and to be successful in completion of this thesis work.

This thesis work would not have been possible without the support of many people. I would like to express my gratitude to my advisor, Dr. Perumalla Janaki Ramulu, who guided me throughout this project. He has been an ideal teacher, mentor, and thesis supervisor, offering advice and encouragement with a perfect blend of insight and humor. I'm proud of, and grateful for, my time working with him.

I would also like to thank Mr. Eliyas Habtu for his support in the experimentations carried out for this thesis.

Table of Contents

List of Tables

List of Figures and Illustrations

List of Acronyms and Abbreviations

APA – Al-sheet – PVC – Al-sheet

FEA – Finite Element Analysis

FLC – Forming Limit Curve

FLC_0 – Lowest point on FLC

FLD – Forming Limit Diagram

GPG – Galvanized steel – PVC – Galvanized steel

GSS – Galvanized Steel Sheet

LDH – Limiting Dome Height

MPM – Metal/Polymer/Metal

PE – Polyethylene

PP – Polypropylene

PU – Polyurethane

PVC – Poly vinyl chloride

WRB – Warm Roll Bonding

Abstract

Metal-polymer-metal (MPM) sandwich composites are in the class of proficient engineering materials which give superb strength-to-weight ratios because of their comparatively low density. These materials are vital constituents within the automobile, aerospace, marine and civil construction industries as substitutes for sheet metals that considerably reduces weight while not compromising functionality. For these materials to be utilized within the aforesaid industries, they need to bear numerous forming processes that are essential in product manufacturing. This thesis investigates formability of metal-polymer sandwich composites made of 'AW 6082– PVC – AW 6082 (APA)' and 'Galvanized steel – PVC – Galvanized steel (GPG)' sandwich sheets, considering epoxy structural adhesive as binding agent, via experimentation and finite element simulation. Tensile strength, plastic-strain ratio (r-value), lowest point on FLC (FLC_0) and adhesive strength are obtained from experimentation. These values are fed into Limiting Dome Height (LDH) simulation (performed using Altair Hyperworks software) for multiple strain path analysis. The results are forming limit diagram (FLD) and dome height at diverse conditions of punch velocity and friction. Aluminum and APA revealed more anisotropic behavior compared to galvanized steel and GPG respectively. A comparison is made to represent the best combinations for formability of the sandwich composites. Maximum formability and dome height (LDH) are attained at low friction conditions (less than 0.015) and forming speed (5000 mm/min). The comparison of FLC_0 values obtained revealed acceptable match between experimental and simulation values. Weight reduction of 9.777 % - for APA – and 27.75 % - for GPG – are achieved compared to aluminum sheet and galvanized steel sheet respectively. The results indicate that the studied MPM sandwich composites can undergo forming operations.

Keywords: Sandwich; Formability; Limiting Dome Height; FLD; Hyperworks

CHAPTER ONE
Introduction

1.1 Background and Description

The need for modern materials arises to cope with the requirements of modern and efficient engineering innovations. Availability of engineering materials that meet design requirements is the major factor that influences engineering design flexibility. Composite materials play a vital role in attaining the aforementioned phenomenon.

Composite materials are made from two or more constituent materials with significantly different physical or chemical properties that, when combined, produce a material with characteristics different from the individual components. This synergistic combination results in new materials stronger, lighter, or less expensive when compared to traditional materials (Babaki and Shakouri, 2019). Composites are preferred over conventional materials in several applications due to their enhanced mechanical, thermal, chemical, and electrical properties.

One of the ways to make composite materials is by formation of Metal-Polymer-Metal (MPM) sandwiches joined together to form composite sheets (Mousa and Kim, 2017). It consists of two metallic skin sheets and a low-density polymeric core material as shown in Fig. 1.1. The polymeric core material offers advantages for weight reduction, lower density, better sound vibration and damping characteristics and improved specific mechanical properties compared to monolithic metallic sheets.

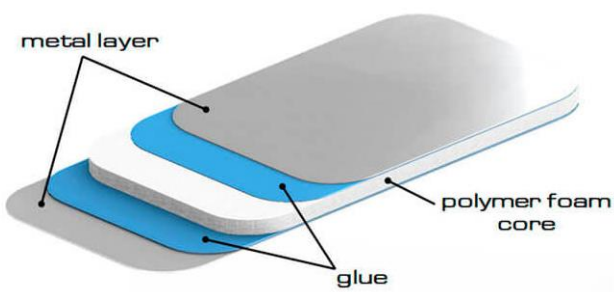

Figure 1. 1: MPM sandwiched composite (Mousa and Kim, 2017)

Metal-polymer-metal (MPM) sandwiched composites are among modern materials which possess the combined properties of distinct materials – from the metal and the polymer – that include low density, significantly higher strength-to-weight ratios and modulus-to-weight ratios, better fatigue strength as well as fatigue damage tolerance than those of monolithic metallic sheets, high specific stiffness and strength, and excellent corrosion properties. These materials enhance engineering design flexibility especially in weight-critical products. They provide preferable properties synergistically combined from both the metal and the polymer, that cannot be obtained from monolithic sheets.

Recent developments in sandwich composites lead to the development of materials that combine the high flexural stiffness and buckling resistance of metals with the low weight of polymers (Harhash *et al*. 2020). These materials have great potential for application in modern lightweight structures. They provide an innovative substitute for the commercial sheets thanks to their lightweight potential with enhanced specific stiffness and thermal and acoustic isolation advantages.

MPM laminate composites are widely used in various industries, including automobile (oil pans, dash panels, and valve covers) to reduce the interior noise and vibration in passenger compartment, aerospace, marine, civil construction, household appliance industry (dishwasher, refrigerators, and air conditioners) to control noise and vibration as passive dampers (Safaei *et al*., 2019).

The adhesion phenomenon plays a role in many instances such as coatings, multilayered sandwiches and composite materials in which the solid components are in contact and should act as an integral structure (Baldan, 2004). Intrinsic adhesion force should be generated through an interface between two components until the optimum adhesion is achieved.

Structural features such as face to core sheet thickness ratio, physical and mechanical properties of the face and core materials, as well as bonding between the layers and the interfacial properties are the main parameters affecting the physical (e.g., sound and vibration damping) and mechanical (e.g., strength and formability) properties of the sandwich sheets (Kim *et al*. 2003).

1.2 Problem statement

Due to the inhomogeneous behavior of the multi-layered sandwich materials over their thickness, several research needs and demands have been concerned with characterizing their forming behavior.

Generally, industrial application of the MPM laminates is restricted due to inadequate information about their property and formability. Accurately predicting the mechanical properties and formability of these materials has been challenging. There is no data about characterization and formability of APA and GPG. Because of the demand for the metallic sandwich sheets, the investigation of their mechanical properties and their forming behavior – taking into account the adhesive strength – when subjected to various forming operations is the main goal of this study.

1.3 Objectives

1.3.1 General objective

The general objective of this thesis is to investigate the mechanical properties and formability of MPM sandwiched composites, considering the effect of adhesion, through experimental and simulation work.

1.3.2 Specific objectives

The specific objectives of this thesis are:

- ✓ To conduct experimentations, tension tests, in-plane stretching, plain strain test, and material characterization and to carefully collect data on mechanical properties of the MPM sandwiched composites as a function of adhesion.
- ✓ To model and perform LDH formability simulations of MPM sandwiched composites and generate FLD using finite element analysis (FEM) tools.
- ✓ To compare findings from the experimentations with the corresponding simulated results and to draw conclusions on the formability of MPM sandwiched composites.

1.4 Scope of the study

In this study, MPM sandwiched composites will undergo basic uniaxial sheet forming experimentations like in-plane stretching and plane straining and their response to these forming operations will be studied. The mechanical properties of MPM sandwiched materials will be examined prior to the forming operations using laboratory Universal Testing Machine (UTM). After studying the effect of adhesives and process parameters on the formability of MPM sandwiched composites, biaxial finite element LDH simulation works will be undertaken to validate the experimental findings. The results will be thoroughly assessed in order to determine the suitable process parameters for forming of MPM sandwiched composites.

1.5 Significance of the study

This thesis will encourage local sheet metal-based industries to consider the usage of MPM sandwich composites since they could become better substitutes. In addition, the forming behavior of these materials specifically considering the adhesive strength will be provided by this thesis as there are limited researches in this area.

Furthermore, several automobile assembly factories are being planted in Ethiopia nowadays. Some components of these automobiles, like roofing, hoods, and doors can be manufactured from these MPM sandwich composites instead of monolithic metallic sheets for the advantages which will be discussed later in the application area.

1.6 Research question

- What are the mechanical properties of MPM sandwich composites?
- What is the effect of adhesion on mechanical properties of MPM sandwich composites?
- Can MPM sandwich composites be formed?
- Which factors contribute to the formability of MPM sandwich composites?

1.7 Limitation of the study

Due to unavailability of warm roll bonding (WRB) setup for fabrication of MPM laminates, hand layup technique is utilized which is susceptible to porosity and defects.

Even though it was intended to study multiple combination of metallic and polymeric materials, it was difficult to obtain flat thermoplastics with the required thickness. Hence, only PVC is utilized. In order to perform multiple strain path formability analysis, limiting dome height (LDH) experimental setup is required. However, since it is not available, single strain path experimentations and LDH simulations have been performed.

1.8 Organization of the thesis

This thesis is organized in five chapters. The first chapter includes introduction which provides back ground of the study, problem statement, objective, scope, significance of the study, research question and limitation of the study. The second chapter covers the review of related literatures. The third chapter discusses about materials utilized and methodology followed for experimentation and simulation works. Chapter four presents the obtained results from both experimentation and simulation with comparison. The final chapter covers conclusions, recommendations, future work, references and appendix.

CHAPTER 2
Literature Review

2.1 Introduction

Sheet metal forming is a well-known and widely used manufacturing process and scientists have done numerous researches in the field. To use MPM sandwiched composites as a substitute to sheet metals, their forming behavior should be well understood. Researches in the manufacturing process of MPM sandwiched composites and adhesives used are also conducted.

In recent years, MPM sandwiched composite materials have attracted remarkable attention to obtain superior properties which do not have any of the layers alone. Metallic sandwich sheets have better strength-to-weight ratio, vibrational damping and sound-deadening properties than monometallic layers (Engel and Buhl, 2011; Babaki and Shakouri, 2019). As a result, Sandwich composites were widely used in the automotive and aerospace industries (Sokolova, Carrado, and Palkowski, 2011; Safaei *et al*., 2019). Sandwich structures are composed of a high strength metallic sheet as the skin layer and thermoplastic or reinforced polymers as the core layer. These laminated structures can be produced by different processes like roll bonding, layup method, and hot pressing (Carrado *et al*., 2010; Mousa and Kim, 2017).

2.2 Materials used in MPM

Various kinds of metallic skin and polymeric core materials are utilized to make MPM sandwich composites. Steel and aluminum and their alloys have been most commonly used as skin materials.

As discussed in (Karlsson and Tomas, 1996) the most common core materials used are expanded polymer foams, which are often thermoset to achieve reasonably high temperature tolerance, though thermoplastic foams are used as well. Almost any polymer may be expanded, but the most common ones in sandwich applications are polyurethanes (PU), polypropylenes (PP), polystyrenes (PS), poly (viny1 chloride) s (PVC), poly (methacry1 imide) s (PMI), poly (ether imide) s (PEI) and polyphenolics (PF). PU may be foamed in situ between the faces and thus does not need to be prefoamed into blocks. In situ foaming thus may eliminate the need to form or machine complex core geometries.

Many kinds of aluminum – plastic sandwich sheets have been developed with different aluminum alloy as skin sheet and different plastic as core layer, such as AA5182-polypropylene-AA5182 sandwich sheet, AA5005-polypropylene-A5005 sandwich sheet, and AA3105-polypropylene-AA3105 sandwich sheets (Kee *et al*. 2009).

2.3 Adhesion

Adhesive bonding is a technique often used in industrial applications. Basically, the process consists of the following steps: (1) surface preparation of adherends by degreasing, grinding etching, or by applying a primer layer for increasing adhesion (Wegman, 1989); (2) joining partners are firmly clamped and adhesive is applied; (3) joining surfaces are brought in contact and kept under pressure; (4) adhesive cures and joint is formed; cure can take place at either elevated or room temperatures.

Joining the metal/polymer/metal sandwich (MPM) is one of the major challenges facing their processing due to the existed polymeric core layer; the core layer is electrically insulating (hinders the welding process), soft (leads to dimension distortion under mechanical joining) and not thermally durable/stable (degrades under elevated temperature processes like welding and some coating processes).

In order to produce a strong and durable adhesive joint between different substrates, surface treatment is necessary. Certain bonding techniques provide adequate static strength, but have little durability when exposed to hot moist environments, while others are susceptible to debonding in the presence of fuels, oils and cleaning solvents commonly encountered in aircraft applications. In addition, the nature of the surface treatment prior to bonding is found to be a major influence in the control of this effect (Shaffer *et al*. 1991). Surface treatment increases the bond strength by altering the substrate surface in a number of ways including increasing surface tension, increasing surface roughness or changing surface chemistry. By increasing surface roughness, an increase in surface area occurs which allows the adhesive to flow in and around the irregularities on the surface to form a mechanical bond. Changing surface chemistry may result in the formation of a chemical bond e.g. between the polymer molecules in the polymer matrix composite and the metal oxide layer on the other adherend surface layer (Clearfield *et al*. 1990).

Adhesive bonding is a solid-state joining technique that relies on the formation of chemical bonds. Thermoset polymer is used for bonding because of its stiffness and resistance to fatigue and heat. For structural applications, if strong enough bonds can be formed, adhesive bonding is preferred over mechanical fastening for its larger joint surface area and lack of need for material removal, which both result in stress concentrations (Magalhaes *et al*. 2004). Adhesives also influence mass reduction strategies by enabling the use of multi-piece assemblies.

Epoxy adhesives are primarily composed of epoxy resin and curing agent. Epoxy adhesives are supplied in both one-component package and two-component package depending on curing agent used and curing method applied. Two-component epoxy adhesives are prepared by packing epoxy composition and curing agent composition separately. They cure soon after mixing the two components together. Almost all room temperature cure epoxy adhesives are supplied in two-component package (Chunfu, *et al*., 2019). One-component epoxy adhesives are prepared and supplied by mixing all formulated components in advance including epoxy resin and curing agent. However, one-component epoxy adhesives usually need cure at elevated temperature and store at low temperature in a refrigerator or even freezer. Epoxy adhesives have been widely used as typical reactive adhesives for various applications ranging from general industry, construction, electronics assembly, automobile production to aerospace market (Chunfu, *et al*., 2019).

Epoxy adhesives show good adhesion on various substrates and are suitable to bond metals, glass, concrete, ceramics, wood and many plastics. Curing shrinkage is very low. Cured epoxy resin possesses strong and rigid cross-linked chemical structure suitable for structural bonding applications (Chunfu, *et al*., 2019). By combination of various epoxy resins and different curing agents, a number of epoxy adhesives have been commercialized for different applications.

For the case of bonding metals and polymers, epoxy adhesive is preferred for its high stiffness and ability to fill small cracks (Guide to Bonding). They have been available for longer than any other engineering adhesive and are the most widely used for structural applications. Epoxy adhesives are two-part resin-hardener system. Once the two components are mixed together, the polymerization process begins, and the polymer begins to harden. Epoxies also have very little shrinkage occur after bonding compared to other adhesives, which is important for reducing stress concentrations. Table 2.1 shows ranges for shear strength values of common thermoplastic adhesives (Magalhaes *et al*. 2004). Of these, epoxy exhibits the highest upper limit by a large margin.

Table 2. 1: Comparison of Common Adhesives (Magalhaes *et al*. 2004)

Adhesive	Shear Strength Range (MPa)
Epoxy	1.00-172
Methacrylate	1.00-32.0
Polyurethane	0.352-19.7
Silicone	0.0827-3.45

Though the adhesive material has a high stress tolerance, the bonds do not resist stress as well. This is evident when comparing the shear strength distributions of the bonds to the peel and cleavage distributions. The stress in the shear loading scenario is distributed at both ends, shown in Fig. 2.1, and does bear much load in the center (Guide to Bonding). The viability of the bond then becomes dependent on the mechanical properties of the adhesive. The cleavage and peel scenarios shown in Fig. 3, however, bear the load almost entirely in the interface of the adherend and the adhesive at the location of the applied load (Guide to Bonding). Once cracking occurs, cleavage and peel stress quickly propagates through the bond causing failure. Failure of the interfacial bonds between the adherend and the adhesive is referred to as adhesive failure, while failure of the adhesive material is referred to as cohesive failure.

Adhesive bonding has proven to be a very effective method for joining dissimilar materials. The primary function of adhesive-bonded joints is the transfer of load by shear (Johnson, 1986). The overall mechanical strength of adhesive bonded joint is, in its majority, dependent on the adhesive properties (strength and ductility), but joint configuration also plays an important role. Adhesive shear stress distribution in an overlap-bonded joint is uneven, where the edges will experience the loading peak values, while the central regions will be less affected. The most used industrial adhesives are the epoxy-based, cyanoacrylates, silicon-based and polyurethanes (Reitz and Oman, 2000).

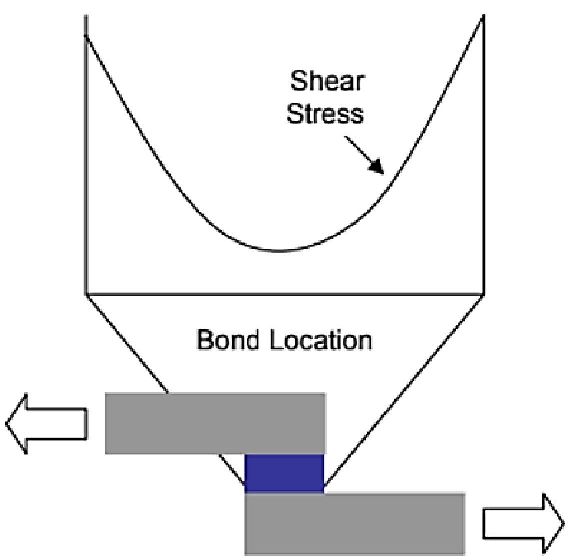

(a) (b)

Figure 2. 1: (a) Shear Stress Concentrations, (b) Cleavage and Peel Stress Concentrations (Guide to Bonding)

2.4 Fabrication of MPM sandwich composites

In order to fabricate the sandwich composites, normally the metallic skins and the core layer are manufactured separately and then the layers bond together (Sokolova, Carrado, and Palkowski, 2011). This process requires to use soft materials as the core layer to form the sandwich sheets conveniently with the manufacturing processes like bending and deep drawing (Sokolova, Kuhn, and Palkowski, 2012).

While the sandwich concept is used in an impressive variety of applications, the techniques employed to manufacture components tend to be few and usually involve a large degree of manual labor. Regardless of material type, the faces and core may be manufactured separately in one step and then bonded together in another step at a later point in time.

Common processes for the production of sandwich structures are adhesive bonding (Sokolova *et al*. 2010), layup method, liquid moulding (resin transfer moulding RTM) (Cochis *et al*. 2013) as well as continuous and discontinuous lamination processes (Karlsson and Tomas, 1997).

Among various manufacturing techniques that have been used to produce metal-polymer-metal sandwich composites such as heat pressing, direct injection molding, over molding, and roll bonding, roll bonding offers advantages of continuous production and cost reduction when compared with other techniques, (Sokolova, Carrado, and Palkowski, 2011). (Mousa and Kim, 2015) introduced a direct adhesion technique by using a warm roll bonding (WRB) process to produce aluminum-polyurethane-aluminum sandwich composites. They investigated the adhesion strength of the layers and found that the dominant bonding mechanism was mechanical interlocking.

2.5 Properties of MPM

The structural sandwich concept involves combining two thin and stiff faces with a thick and relatively weak core. By sandwiching the core between the two faces and integrally bonding them together, a structure of superior bending stiffness and low weight is obtained. Since the core often has exceptional insulative properties, the entire sandwich structure may further be characterized by excellent thermal insulation and also acoustic damping at certain frequencies (Kim *et al*. 2003).

The strength of the sandwich is determined by the mechanical properties of the polymer, the metal and their interfaces. Polymer and metal differ significantly in their mechanical behavior, especially in their values of strength and ductility, and the MPM behave quite differently compared to the monolithic materials under similar load conditions (Harhash *et al*. 2014). Hence it is not only important to study the mechanical behavior of the individual bulk materials, but also to study their deformation behavior as a hybrid.

The MPM sandwich composites are three-layered multi-material laminates joined together with the help of adhesives into one integral part and these constituent materials (aluminum and galvanized steel sheets, PVC and epoxy adhesive) have different thermal properties. It is not the purpose of this thesis to extensively study the thermal behavior of MPM sandwich composites. However, the temperature range in which these materials can operate and their expansion and conductivity in that range should be extrapolated from the constituent materials' thermal properties. The thermal behaviors of aluminum, galvanized steel, PVC and epoxy adhesive are tabulated in Table 2.2.

Table 2. 2: Thermal behaviors of aluminum, galvanized steel, PVC and epoxy adhesive (Materials Thermal Properties Database)

Material	Aluminum	Galvanized steel	PVC	Epoxy adhesive
Thermal conductivity (W/mK)	237	80.4	0.15	0.14
Linear thermal expansion coefficient, α at 20 °C ($x10^{-6}$ K^{-1})	23.1	12.3	52	32.51
Melting point (°C)	660.32	1410	214	177

From the above table the following points can be extrapolated.

- Even though aluminum and galvanized steel have a relatively high thermal conductivity values, the sandwiched polymers have very low values of thermal conductivity. As a result, heat is barely conducted across the surface of MPM sandwich composites (have insulative characteristics).
- On the other hand, the polymers have relatively higher linear thermal expansion coefficient (α) than those of the metallic counterparts (when they are free from physical constraints). However, the three layers have been strongly bonded (by epoxy adhesive layers at interfaces) as one integral part (meaning, there is a physical constraint applied). Hence, the MPM sandwich composite can expand only by the smallest α-value among the four components.
- The lowest melting point among the four constituent components determines the maximum temperature that the MPM sandwich material is operable. Since the strength of epoxy adhesive degrades beyond 177 °C, the MPM sandwich composites (with epoxy as an adhesive) should be used in the range of room temperature to 177 °C.

2.6 Formability of MPM

Although the metal–plastic sandwich sheets have many advantages, the forming of these materials is very complicated due to the extremely large difference in mechanical properties and in the gauges of polymer core and the metal skins. The behaviors of the sandwich sheets are quite different from those of homogenous metallic sheets during forming processes. The interface stress between skin sheet and core layer has a large influence on the deformation behavior of sandwich sheet (Makinouchi, 1988). Furthermore, the sliding and shearing occur between skin sheet and core polymer hence affect the formability of the sandwich sheet. Investigating its formability will play an important role on improving the application of metal–plastic sandwich sheet.

Metal–polymer–metal (MPM) sandwich composites are characterized by high deformation potential that makes them suitable to be formed in complex shapes. (Kim *et al*. 2003) have shown that AA5182/polypropylene/AA5182 sandwich panels, characterized by formability and strain rate sensitivity higher than those exhibited by the aluminum sheet, allows the obtaining of complex structures for automotive applications. Since the mechanical properties and formability of metals significantly differ from those of polymers, the MPM sandwich structures are characterized by different properties with respect to constituent materials. To this purpose, (Harhash *et al*. 2014) have shown that the strain hardening exponent and strength coefficient of 316L/polypropylene–polyethylene/316L sandwich decrease as compared to the ones measured on the monolithic steel sheet due to the contribution of the soft core on the strengthening behavior of the MPM sandwich.

Forming processes of parts in MPM sandwich usually involve issues, such as wrinkling, delamination, and shearing, related to the inadequate interlayer metal–polymer adhesion. The adhesive strength at the metal–polymer interfaces is a key factor for MPM sandwich composites since the interfacial interaction generates a system that can strongly affect the sheets to either act independently, weakly, or as strongly coupled. A weak polymer core can act as a lubricant between the metal skins; such behavior can cause the occurrence of debonding at interfaces between sheet and plastic core, leading to a sliding of metal skins and a premature failure during forming operations. On the other hand, a too strong adhesion force between polymer core and metal sheet can negatively affect formability since the continuous smooth sliding between layers is prevented (Ruokolainen and Sigler, 2008 and Stachowiak and Batchelor, 2014). Furthermore, as reported by (Kim and Yu, 1997), the bonding between dissimilar materials to obtain a multi-layer component generates inhomogeneities leading to discontinuities in stress distributions across the sheet thickness. A further drawback taking place during forming processes of sandwich composites is the higher tendency to wrinkle with respect to the monolithic metal sheets. This is due to the weak interlayer adhesion that, allowing the two metal sheets to act independently, make them be more susceptible to wrinkling than a single thicker sheet. Also, delamination can occur during forming operations due to the different lengths of the metal skins, as they are deformed around the die, which can cause the occurrence of high shear forces in the polymer core (Ruokolainen and Sigler, 2008 and Wollmann, 2017). (Harhash *et al*. 2020) analyzed the effect of the polymer core thickness on spring back of steel–polymer–steel sandwich composites; they showed a reduction in spring back with decreasing core thickness even though, with thicker polymer films, crack probability rises due to the increase in tensile stresses on the outer metal skin. Furthermore, as shown by (Carrado *et al*. 2011), the presence of cavities in the polymer core, caused by air bubbles trapped during the manufacturing process of sandwich laminates, can accelerate cracking. Factors, such as the inhomogeneous cross-section structure of multi-layer sandwiches, composition and characteristics of the different constituents, bonding method used to hold together the single layers, shape complexity of the final component, forming technique as well as loading conditions, can strongly affect the success of forming processes of multi-layer materials and, consequently, the final performances of the formed parts.

Forming of these multi-layered sheets face some obstacles due to the inhomogeneous cross-section structure, where their forming limit depends on the mechanical and geometrical properties of the skin and core layers and additionally the shear strength between them. The shear strength between the used components, as discussed in (Harhash *et al*. 2016), is enough to guarantee delamination-free forming in all cases examined.

Due to the need to form structures of even complex shapes out of a raw sandwich material, the investigation of the forming behavior of those materials is an area of special interest. They of course show a different forming behavior compared to the mono-materials used, e.g., an inhomogeneous cross sectional stress distribution as a result of bonding dissimilar monolithic sheets together (Kim and Yu, 1997).

Laminated metal/polymer materials show an acceptable or even good formability. For instance, Hylite, an Al/PP/Al-sandwich (Burchitz *et al*. 2005), exhibits a good shaping behavior under deep drawing or bending conditions. Other examples on the steel-based sandwich are Litecor (ThyssenKrupp, 2012) and steel/PP–PE/steel (Harhash *et al*. 2014).

FLD is a curve that shows the maximum strains that a sheet can tolerate without any necking (Ghazanfari *et al*., 2019; Alipour *et al*., 2019). (Parsa, Nasheralahkami, and Ettehad, 2010) studied the spring back behavior of AA3105/polypropylene/AA3105 laminated sheets numerically and experimentally. (Harhash *et al*., 2014; Harhash, Carrado, and Palkowski, 2017) analyzed the mechanical properties and formability of the steel/polymer/steel sandwich composites in stretch forming and deep drawing processes. (Mousa and Kim, 2017) investigated the mechanical properties of the laminated sandwich sheets of AA1100/polyurethane/AA1100 at various thickness reduction. The FLD of the sandwich sheets with aluminum as the skin layers and glass fiber reinforced polymer as a core was predicted numerically and experimentally by (Aghchai and Khatami, 2018). They utilized the M–K model to predict the FLD numerically. The study on the effect of the variation in thickness of the core and skin layers revealed that the increase in the thickness of both skin and core layers improves the FLD of the sandwich sheet but variation in the thickness of the skin layers has a greater effect on the formability. Also, (Keipour and Gerdooei, 2019) studied the spring back behavior of the aluminum/reinforced polymer sandwich composites. The results show that for thicker cores, a reduced spring back could be stated.

(Dicello, 1980 and Link, 2001) experimentally studied the formability of steel/ polypropylene/steel sheets. They conducted different types of experiments such as deep drawing, hole expansion, cutting, and hemispherical punch stretching on sandwich sheets with different thicknesses of layers. The results of these experiments showed that, the sandwich sheets present superior formability over single-layer steel sheets. Similar investigations on three-layer aluminum 5182/polypropylene/aluminum 5182 sheets resulted in comparable conclusions (Kim *et al*. 2008). (Sokolova *et al*. 2010) analyzed formability of sandwich sheets whose skin layers were made from dissimilar materials (aluminum and steel). They conducted Ericson and deep drawing tests on the sheets, finding lower formability for sandwich sheets with dissimilar skins rather than those of two steel skins. In a similar study, the effect of polymeric core layer thickness on the formability of steel/polymer/steel sheets were studied (Sokolova *et al*. 2012). It was observed that, die geometry and the thickness of the core layer have significant effects on the sheet fracture. (Harhash, 2015 and Palkovski, 2014) studied the behavior of the steel/polymer/steel sheets during cylindrical cup drawing. They constructed FLC of the sheet using surface strain calculations. (Kami *et al*. 2017) studied the formability of Bondal sheets (a three-layer steel/polymer/steel sandwich sheet) by conducting different types of experiments such as Nakazima, uniaxial tensile and bulge tests. In addition to the above-mentioned experimental studies, many attempts have been made to analyze the formability of sandwich sheets following numerical and theoretical approaches. (Kim *et al*. 2003) calculated FLCs of aluminum/ polypropylene/ aluminum sheets using a M-K model whose properties were equivalent to those of the considered sandwich sheet. Similar investigations were done by (Somayajulu 2004). Later on, (Kim *et al*. 2015) developed a M-K model for determining FLCs for sandwich sheets. The developed M-K model accepted mechanical properties of each layer separately. The authors assessed the effect of layer thickness and material on FLC of the sandwich sheets. The possibility of improving formability of sandwiches by adopting layers of dissimilar materials have also been studied. (Kami *et al*. 2016) predicted FLC of the Bondal sheet using an anisotropic model.

2.7 Application of MPM

Formerly, deep drawn components were mostly manufactured by using sheet metals like Stainless steel (Padmanabhan *et al*. 2007, Chen and Lin, 2007, Gorji *et al*. 2011, and Yazdi *et al*. 2017), Copper (Gorji *et al*. 2011, and Yazdi *et al*. 2017), EDD (extra deep drawing material) (Takalkar *et al*. 2015), and Brass (Dhaiban *et al*. 2014) which possesses high strength and heavyweight. Due to the heavyweight, such components were responsible for reducing efficiency when used in the automobile and aerospace industries. Many scientists tried to overcome this problem by replacing single metal sheets with sandwich composite sheets, which possess high strength and low weight. The forming of such sandwich composite sheets depends on the type of sandwiched metal sheet, bonding process, geometry, and parameters (Takalkar and Babu, 2018). The prediction of such sandwich composite sheets' formability is difficult, particularly when the two skin metal sheets are dissimilar with different formability. The generation of FLD overcame this problem.

In automotive industry, in order to reduce the weight of whole car, steel–plastic sandwich sheet have been used to manufacture some automotive components which were formed by the single steel sheets, such as dash panel, and wheel house inner (Yao *et al*. 2003). Compared with steel–plastic sandwich sheet, aluminum–plastic sandwich sheets provide a lower weight per square meter and higher specific flexural stiffness (Veenstra, 1993). Many kinds of aluminum–plastic sandwich sheets have been developed with different aluminum alloy as skin sheet and different plastic as core layer, such as AA5182-polypropylene-AA5182 sandwich sheet, AA5005-polypropylene-AA5005 sandwich sheet, and AA3105-polypropylene-AA3105 sandwich sheets. Among these sandwich sheets, AA5182-polypropylene-A5182 sandwich sheet have been developed for potential application of these materials for automotive body panels in future high-performance automobiles with significant weight reduction (Kee *et al*. 2009).

2.8 Literature Summary and Research Gap

Researches that focus on development/fabrication, properties, formability and usage of MPM sandwich composites have been reviewed in the preceding section. Materials used in MPM composites mostly include aluminum, steel and their alloys – as metallic layer – and PVC, PU, PP and PE – as polymeric core. Joining these dissimilar materials – metal and polymer – is achieved via adhesion using epoxy, methacrylate, polyurethane and silicon. Of these, epoxy exhibits the highest strength.

Besides the mechanical characteristics materials involved, interfacial adhesion strength plays a vital role in the formability and performance of MPM sandwich composites. The aforementioned researches don't give enough emphasis to the effect of this interfacial property. Furthermore, the combined effect of process parameters and material properties on formability of MPM sandwich composites is not addressed sufficiently.

CHAPTER 3
Materials and Methodology

3.1 Materials

The materials selected for this study are MPM sandwiches comprised of aluminum sheet (Al-sheet) with poly vinyl chloride (PVC) and galvanized steel sheet (GSS) with PVC. The metallic skin sheets – Al-sheet and GSS – are purchased from local sheet metal vendors. Although it was difficult to find flat polymeric material within the required thickness, eventually PVC (a polymer of vinyl chloride monomers) sheets were found which meet the criteria. The mechanical properties of PVC enhance with the molecular weight increasing but decrease with the temperature increasing.

Commercial aluminum sheet of thickness 1 mm is one of the metallic sheet components for the MPM laminate composite. The other metallic sheet is made from galvanized steel which is zinc coated for anti-corrosion purpose, and has a thickness of 0.5 mm. The thermoplastic PVC sheet also has a thickness of 0.5 mm.

As an adhesive agent, a two-component 'Hardex' epoxy adhesive, shown in Fig. 3.1 below, which have a 30-minute curing time at room temperature, is utilized in preparation of samples for experiments undertaken for this thesis.

Figure 3. 1: Hardex Epoxy Adhesive

Curing is achieved by reacting the epoxy with polyfunctional curatives or hardeners. A one-to-one ratio of resin and hardener is used. It has moderate viscosity (10 Pa.s) which offers convenient dispensing, and is widely used in many bonding and sealing applications.

3.2 Fabrication

Hand layup technique is used to fabricate MPM sandwich laminates in this study. The surfaces of raw materials, metallic and polymeric sheets, are preprocessed by abrading with sand paper and cleaning with ethanol so that composite laminates of APA and GPG have better bond strength. After the surface preparation, epoxy adhesive is applied at their interfaces and sufficient clamping pressure is applied until the adhesive completely cures. Finally, the dissimilar materials are joined together and become an integral part.

3.3 Methodology

Forming operations consist of simple bending, to stretching to deep drawing of complex parts. The mechanical properties of the sheet material greatly influence its formability. Formability is a measure of the amount of deformation a material can withstand prior to fracture or excessive thinning. Determining the extent to which a material can deform is necessary for designing a reproducible forming operation. This study follows the methodology shown in the following flow diagram.

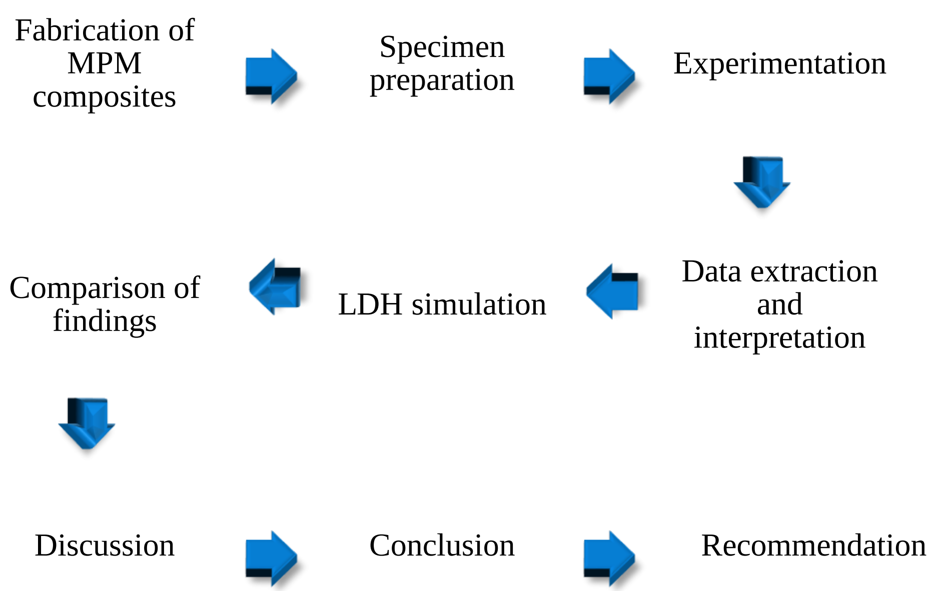

3.4 Uniaxial tensile test

Uniaxial tensile tests are performed on the samples using a Universal Testing Machine (UTM). In the tensile test, the samples were pulled until they break to determine the Ultimate Tensile Strength (UTS) and yield strength (σ_y) of the base materials and sandwich composites. The amount of load applied to the specimens and their corresponding elongation were measured throughout the testing process. The output properties of MPM sandwich samples were expressed in terms of stress, which is the ratio of applied force to cross-sectional area and strain, which is the ratio of change in length to original length.

3.4.1 Specimen preparation

Each test sample for tensile test experimentation is fabricated in three distinct steps. First, in accordance with ISO 6892-1 2016 specification, the flat dog-bone shape adherends are cut-out from polymer sheet and sheet metal blanks as shown in schematic representation, Fig. 3.2. Next, their surfaces are aptly prepared for adhesion with cleaning, abrasion etc. with the aim of increasing their surface energy for better adhesion. Finally, the adhesive is applied at their interfaces and the sandwich is clamped until the adhesive completely sets. These samples will be prepared from three different rolling directions (0^0, 45^0 and 90^0) of the metal sheets in order to consider the anisotropy effect.

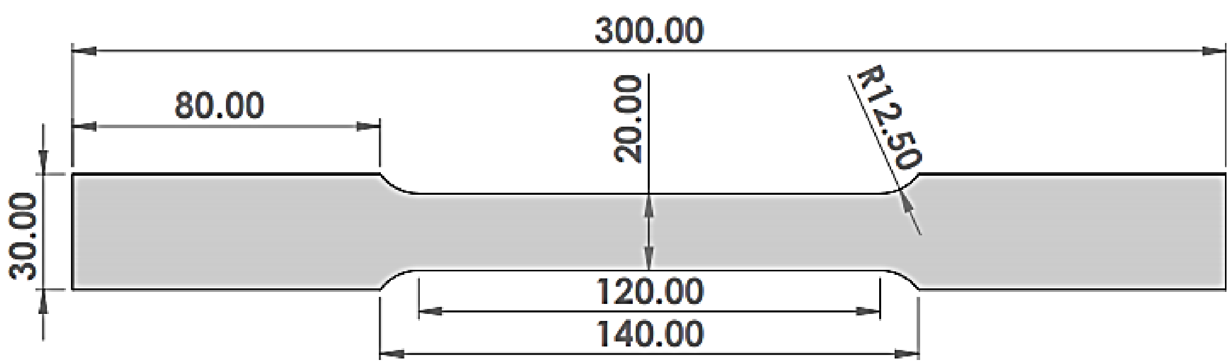

Figure 3. 2: Schematic representation of tensile test specimen [Dimensions in mm] ***(ISO 6892-1 2016 specification)***

3.4.2 Experimental setup

Each pre-fabricated sample for the uniaxial tensile test is discretely tested on the UTM. For this research two UTMs have been used – one in ASTU campus and the other in ETU campus – based on the gripping force and load requirements. The samples were suitably mounted on calibrated UTM with proper alignment and sufficient gripping force as shown in Fig. 3.3.

The top gripper will move a constant crosshead speed which continues till failure of the specimen. The force applied versus the sample’s elongation was continuously monitored and plotted on a stress strain curve until fracture. Measurements like UTS, yield strength, and initiation of necking were calculated once the tests are complete. The broken samples were placed back together to measure their length just before failure and their maximum strain can be obtained via comparison with their original lengths. Similarly, reduction in their thickness is assessed.

3.4.3 Stress and strain

While the deformation was taking place, applied tensile load and material movement (elongation and thickness change) data was being continuously recorded. Engineering stress and strain results can be obtained using equations 3.1 and 3.2 respectively. The result will be plotted graphically in stress-strain curve.

$$\sigma = \frac{F}{A} \quad \text{(3.1)}$$

$$\varepsilon = \frac{\Delta l}{l_0} \quad \text{(3.2)}$$

Where: σ = engineering stress (MPa)

ε = engineering strain

F = force

A = initial cross-sectional area

Δl = change in length = [final length (l) – initial length (l_0)]

Material composition tests have been performed in Adama Steel factory and the obtained compositions of the base materials are illustrated as follows in the Tables 3.1 and 3.2 below. The chemical composition of galvanized steel matches to ASTM A 653 standard. Whereas, the chemical composition of aluminum matches to EN573-3 (EN AW-6082) standard.

Table 3. 1: Chemical composition (%) of galvanized steel – iron makes up the remaining percentage

Fe	C	Mn	P	S	Cu	Ni	Cr	Mo	V	Ti	Zn
Bal.	*0.1*	0.6	0.03	0.035	0.25	0.2	0.15	0.06	0.008	0.025	1.02

Table 3. 2: Chemical composition (%) of aluminum – aluminum makes up the remaining percentage

Al	**Si**	**Fe**	**Cu**	**Mn**	**Mg**	**Cr**	**Zn**	**Ti**
Bal.	0.7-1.3	max. 0.5	max. 0.1	0.4-1	0.6-1.2	max. 0.25	max. 0.2	0.06

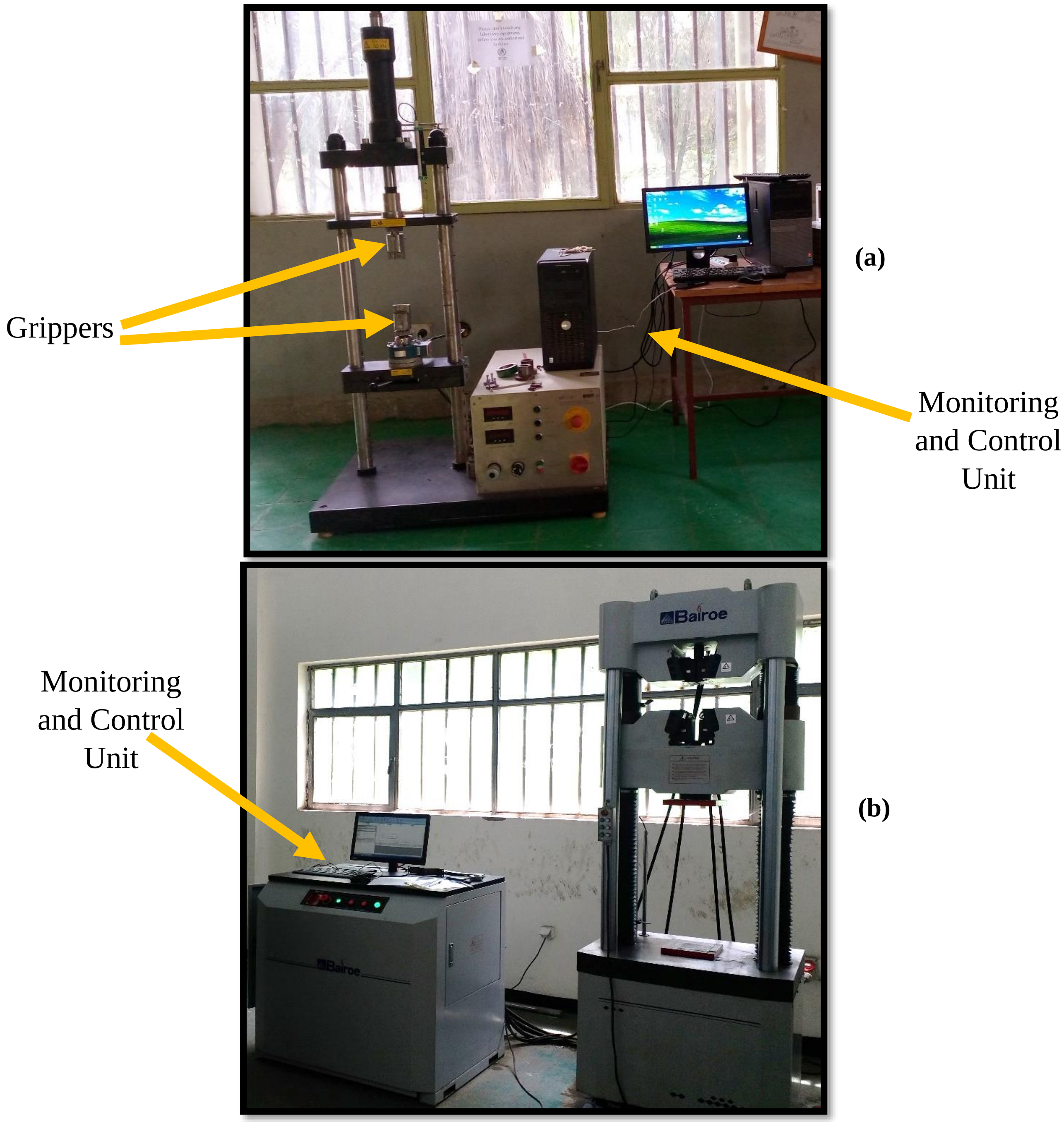

Figure 3. 3: UTM Setup – in ASTU (a), in ETU (b)

The true stress and strain can be related with their engineering stress and strain counterparts using equations 3.3 and 3.4 respectively.

$$\sigma_t = \sigma \frac{l}{l_0} = \varepsilon * (1 + \varepsilon) \quad \text{.....(3.3)}$$

$$\varepsilon_t = \ln{(1 + \varepsilon)} \quad \text{.....(3.4)}$$

Where: σ_t = true stress (MPa)

ε_t = true strain

3.5 Strain hardening

Work hardening, also known as strain hardening or cold working, is the increment in strength of a material while undergoing plastic deformation. Dislocation generation and dislocation movements, within the crystal structure of the material, are responsible for this strengthening.

Before work hardening, the lattice of the material exhibits a regular, nearly defect-free pattern (almost no dislocations). As the material is work hardened it becomes increasingly saturated with new dislocations, and more dislocations are prevented from nucleating (a resistance to dislocation-formation develops). This resistance to dislocation-formation manifests itself as a resistance to plastic deformation; hence, the observed strengthening.

For metal deformation, the strain hardening phenomenon is explicated by Hollomon's equation as follows:

$$\sigma_t = K{\varepsilon_t}^n \quad \text{.....(3.5)}$$

Where: σ_t = true stress

K = strength coefficient

ε_t= true strain

n = strain hardening exponent

Formability of a sheet metal is subject to its strain hardening exponent (n) value. Larger value of strain hardening exponent (n) corresponds to better formability since those materials can withstand larger deformation prior to initiation of necking.

3.6 Yield criterion

When a material is subjected to large plastic deformations the grain sizes and orientations change in the direction of deformation. As a result, the plastic yield behavior of the material shows directional dependency. Under such circumstances, the isotropic yield criteria such as the von Mises yield criterion are unable to predict the yield behavior accurately.

In this thesis work, Hill yield criterion is utilized since it accounts for anisotropic plastic deformations and variations of these criteria are in wide use for metals, polymers, and composites.

For LDH simulations in the FEM analysis, the Hill yield criterion is used while assigning material properties for the MPM sandwich composites.

3.7 Plastic Strain Ratio

Plastic strain ratio (r) is a measure of the ability of a sheet metal to resist thinning or thickening when subjected to a tensile or compressive force. Plastic anisotropy arises due to the preferred orientation of grains in a polycrystalline material and is usually characterized by the r-value, a weighted average measure of the width-strain to thickness-strain ratio in tensile tests conducted along the longitudinal, transverse, and diagonal directions. It is typically advantageous if the material reduces in area a minimal amount when subject to this force, meaning a good drawing material has a high r-value. It is considered a direct measure of sheet material drawability and is useful for evaluating materials intended for forming shapes by a deep-drawing process.

Once the material is taken beyond its elastic limit, it has deformed. If this flows easily in the plane of the sheet it will result in a high r-value. Alternatively, if it flows from the materials thickness it will thin during drawing, which may result in weakness.

To determine this ratio, assuming constant volume, both the axial and transverse strain needs to be obtained during a uni-axial tensile test. The plastic strain ratio (r), is given by:

$$r = \frac{\varepsilon_w}{\varepsilon_t} \quad \text{……………………………………………………………………………………}(3.6)$$

Where: true width strain (ε_w) = ln(w_f / w_0),

true longitudinal strain (ε_t) = ln(t_f / t_0),

w_f = final width,

w_0 = original width,

t_f = final thickness,

t_0 = original thickness.

Equation 3.6 tells us that the r-value is dependent on the ratio of width and thickness changes as the sample is pulled in tension. The word “plastic” in the plastic strain ratio name implies that the specimen is pulled beyond its elastic limit and that only the strain that induces plastic flow is considered in the calculation. Because it is very difficult to accurately measure changes in thickness, we assume the volume of the specimen remains constant and express the longitudinal strain as:

$$r = \frac{\ln\left({}^{W_0}/_{W_f}\right)}{ln\left({}^{L_f W_f}/_{L_0 W_0}\right)} \quad \text{.....(3.7)}$$

Where: L_f = final length

L_0 = original length

Equation 3.7 enables the plastic strain ratio (r) to be calculated manually by measuring the change in axial gage length and the change in width. In this manual approach, prior to testing the specimen width and distance between gage marks is measured with calipers. The specimen is then pulled to a strain less than at maximum force (before onset of necking) and then unloaded. The final width and gage length are then measured to determine r-value.

A material that exhibits unequal properties when tested in different directions is said to be anisotropic. Anisotropy is caused by mechanical fibering due to the directionality of the rolling process. Anisotropy is, more importantly, also caused by preferred crystallographic orientation or ‘texture’ in the material.

Using the r-values in three directions (0^0, 45^0, and 90^0 to the rolling direction), two other important parameters can be calculated (Esther, 2017). ‘Planar anisotropy parameter’ (Δr), which is an indicator of the ability of a material to demonstrate a non-earing behavior (lower is better), can be calculated using equation (3.8). ‘Normal anisotropy parameter’ (r_m), which is an indicator of the ability of a material to be deep drawn (higher is better), can be calculated by equation (3.9).

$$\Delta r = {(r_0 + r_{90} - 2r_{45})}/{2} \quad \text{...3.8)}$$

$$r_m = {(r_0 + r_{90} + 2r_{45})}/{4} \quad \text{..(3.9)}$$

3.7.1 Experimental Setup

The samples for plastic strain ratio (r-value) determination test are prepared as per ASTM-E517 standards (as shown in Fig. 3.4). It is achieved through stretching axially on a UTM. Four symmetrical markings (with a permanent marker) have been applied on the test samples prior to testing (as shown in Fig. 3.5), so that the change in length between these markings are measured after the stretching test.

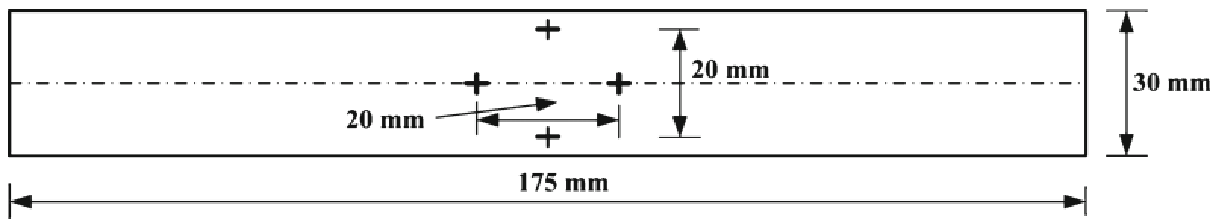

Figure 3. 4: Schematic of plastic strain ratio test sample (ASTM-E517 standards)

(a)

(b)

Figure 3. 5 MPM specimens for r-value test; APA (a), GPG (b)

3.7.2 Experimental procedure

1. Preparation of the MPM composite samples as per the specification and marking dots carefully on their surfaces.
2. Mounting the specimens on the UTM and stretch the specimens up to 10% elongation of the original length.
3. Dismount the specimens and measure the length and width change between the dots.
4. Insert the obtained values in the equation 3.7 and calculate the r-value.

3.8 LDH Simulation

Hecker and Ghosh (1975) proposed Limiting Dome Height (LDH) Test to avoid the small area of deformation which was one of the limitations of the Erichsen cup test, and modified it to simulate plane-strain condition where 80% of stamping failure occurs. LDH test uses 101.6 mm diameter of the punch and sheet material is stretched in biaxial directions while clamped at the edges by lock-bead to avoid draw-in (as shown in Fig. 3.6). This LDH test can be used to evaluate lubricants and interface friction conditions in addition to analysis of forming limits.

FE simulations for the LDH test indicates that the test is very sensitive to friction and it affect the test measurements. Friction at tool-workpiece interface has an effect on formability and thinning distribution. It can be expected that maximum thinning when friction is zero occurs at the apex of the dome. Generally, location of maximum thinning moves away from the apex of the dome (moves toward die corner radius) as interface friction increases, and punch force also increases as interface friction increases (Yoon, 2012).

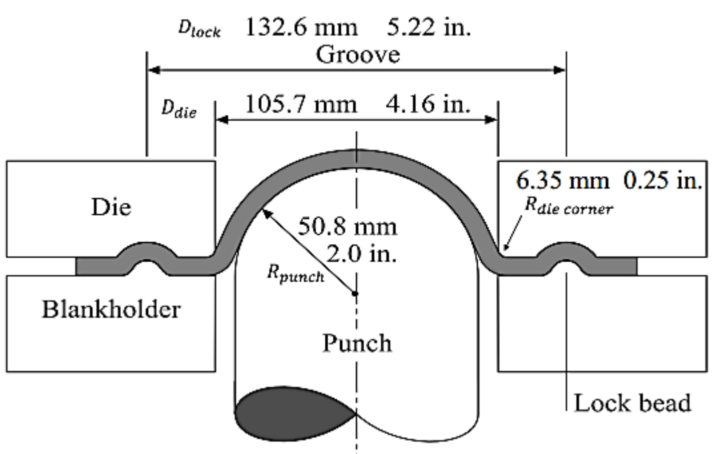

Figure 3. 6: Schematic of LDH tooling (Yoon, 2012)

The LDH simulation replicates the aforementioned experimental testing process with finite element method approach. Altair Hyperworks software have been utilized to perform finite element analysis on the MPM sandwich composites. The Limiting Dome Height Test have been simulated in radioss-incremental solver (one of the numerous solvers in Hyperworks software which is suitable for LDH).

3.8.1 LDH Simulation Procedure

The simulation setup has four main components that are modelled in accordance with their properties – namely, Hemispherical dome shaped punch, blank (MPM sandwich composite sheet), blank holder (binder) and die-cavity. Among these, the punch, binder and die are made rigid components while the blank (MPM sandwich sheets) are deformable with their mechanical properties (obtained from the tests, like tensile strength, r-values, n-values etc.) fed into the model. The lock-bead is imitated by a fixed edge constraint applied on the MPM sheet such that it can't be drawn into the die cavity (pure stretching takes place).

These four components are modelled and assembled using Solidworks 2021 CAD software. The LDH experimental tooling – hemispherical punch, binder and die – are modelled as per the specification. The blanks – on the other hand – are modelled so as to consider different strain paths as shown in Fig. 3.7. These geometries are also taken from the experiment specifications. The friction coefficient values – in dry and lubricated conditions – at the interfaces have been obtained from an archive coefficient of friction (Friction Factors - Coefficients of Friction) and it is varied from zero up to these points for both materials. To observe the effect of forming speed on the materials' formability, an extremely large gap between punch velocities have been assigned for different cases. Various combinations of these process parameters have been assessed in order to find out the optimum conditions for both materials.

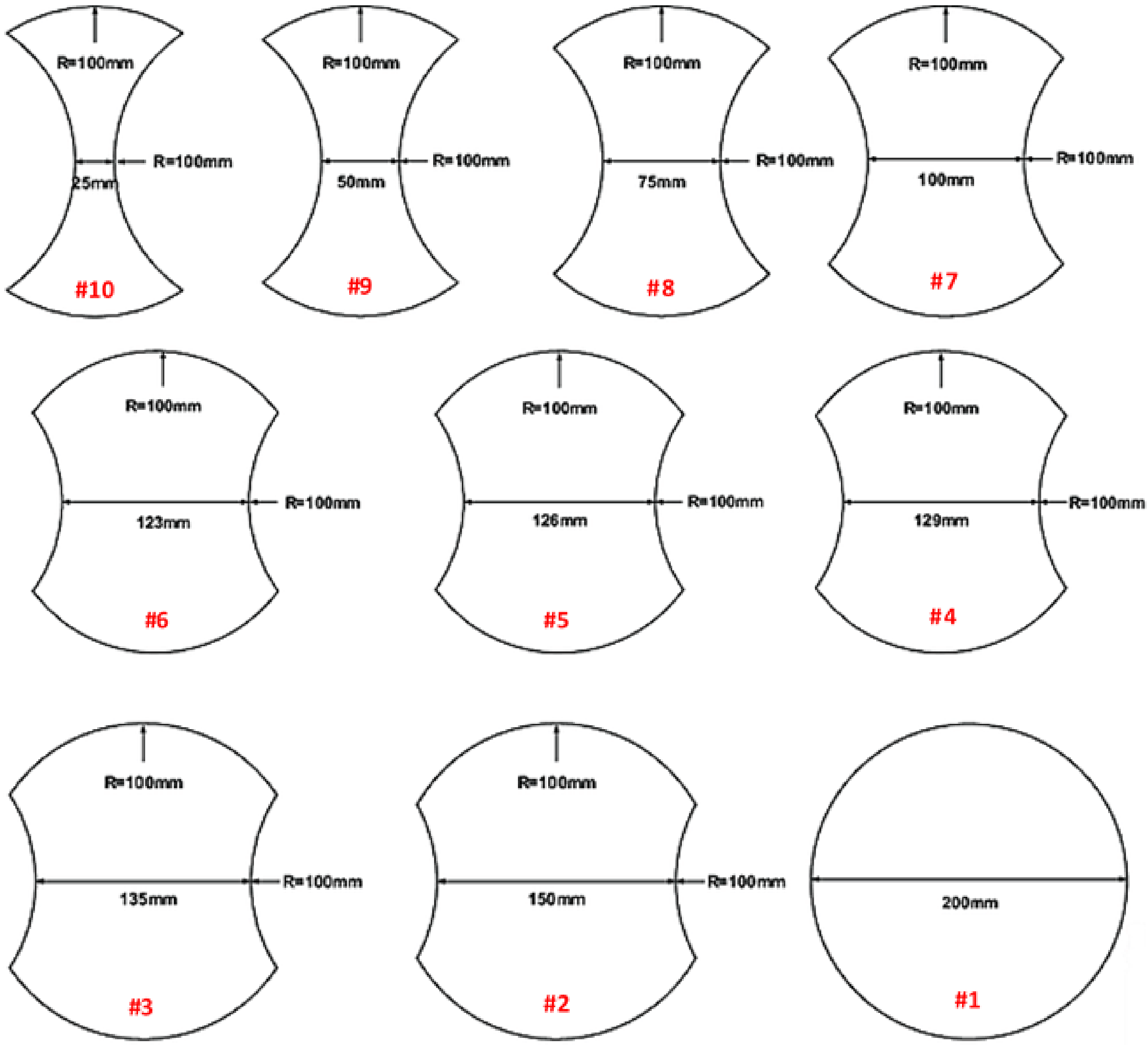

Figure 3. 7: Blank geometries

These models are then imported into the Hyperworks' working environment and meshed appropriately. Subsequently, properties of each respective component are prudently incorporated, as tabulated in Table 3.3, in the pre-processing stage. The LDH setup on the graphics area is shown in Fig. 3.8. below.

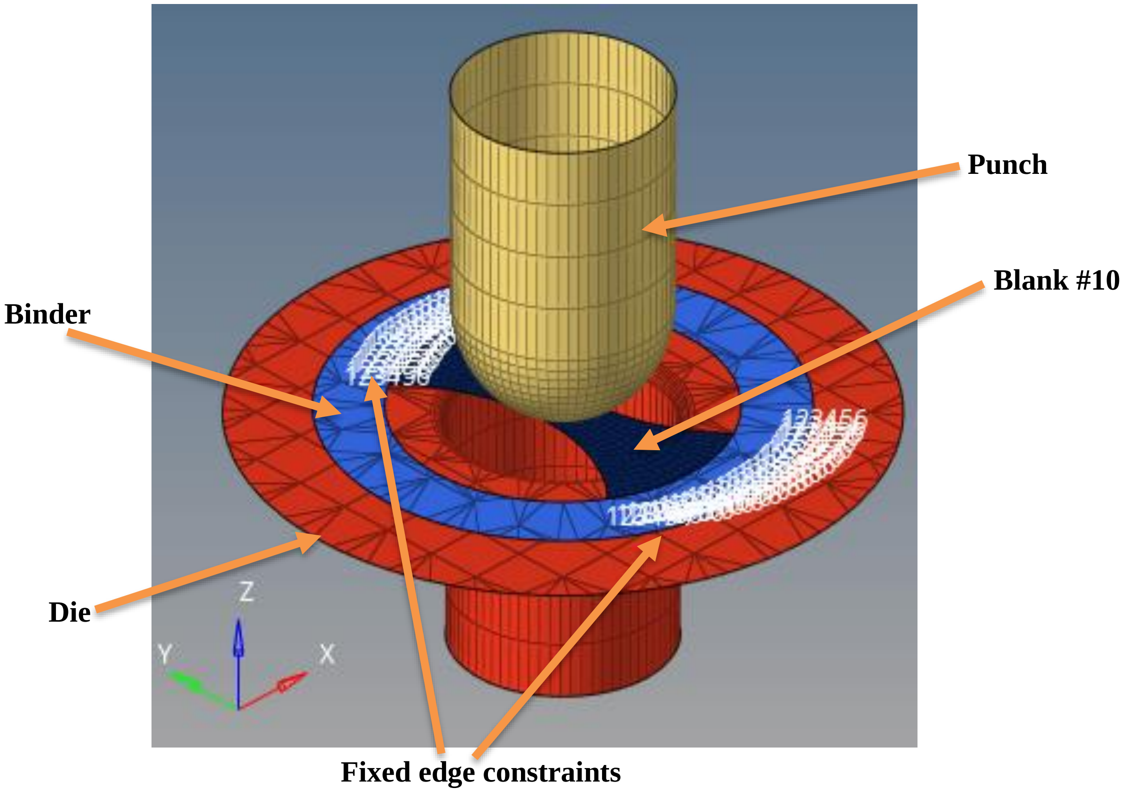

(a)

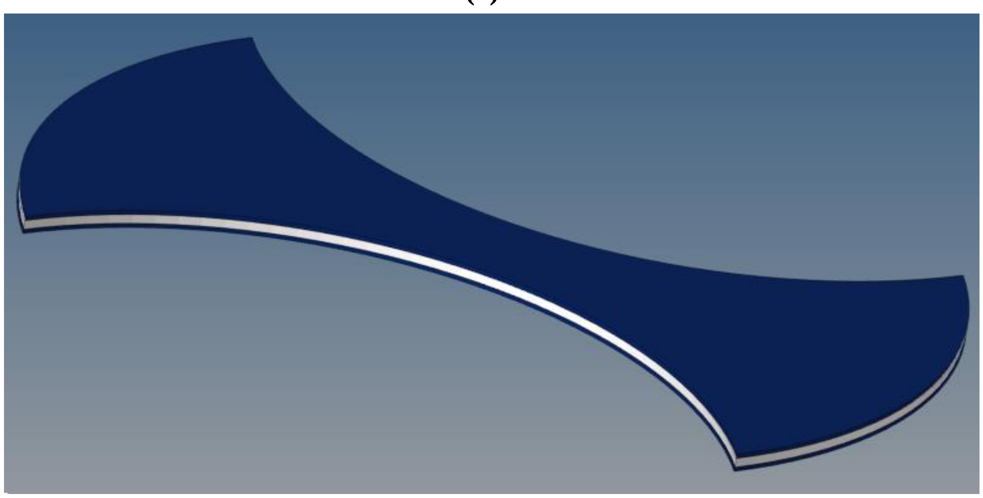

(b)

Figure 3. 8: (a) LDH Simulation setup, (b) blank #10 – the three layers of ply laminate

Table 3. 3: Blank material properties

Blank Material	APA	GPG
Thickness (mm)	1.5	2.5
Yield Strength, σ_y (MPa)	314.43 ± 9.74	648.13 ± 14.54
UTS (MPa)	333.66 ± 8.42	701.57 ± 10.82
Young's modulus, E (GPa)	137.9 ± 8.95	406.82 ± 9.37
R_0	1.1167 ± 0.29	1.6467 ± 0.22
R_{45}	0.9502 ± 0.1	1.476 ± 0.17
R_{90}	1.2908 ± 0.38	1.813 ± 0.05
Strength coefficient, K (MPa)	475.1 ± 15.776	958.04 ± 20.458
Hardening exponent, n	0.25 ± 0.05	0.2 ± 0.02

The surface-to-surface explicit contacts were defined by using penalty function, and the coefficient of friction was assigned between tools and sample. The adhesive layer's contacts between skin Al, Galvanized steel sheets and PVC core were defined by using ply laminates. The generated mesh model was further utilised for the explicit analysis, which carried out in two different stages. In the first stage, the sandwich composite blank was pressed over the die by applying force using the blank holder whereas in the second stage, the pressed blank was further formed by applying force using the dome shaped punch.

3.8.2 Mesh Density

The basic idea of finite element analysis (FEA) is to make calculations at only limited (Finite) number of points and then interpolate the results for the entire domain (surface or volume). Any continuous object has infinite degrees of freedom and it's just not possible to solve the problem in this format. Finite Element Method reduces the degrees of freedom from infinite to finite with the help of discretization or meshing (nodes and elements).

In finite element analysis (FEA), the accuracy of the FEA results and requested computing time are determined by the finite element size which provides mesh density (Yucheng Liu and Gary Glass, 2013). According to FEA theory, the FE models with fine mesh (small element size) yield to highly accurate results but may take longer computing time. On the contrary, those FE models with coarse mesh (large element size) may lead to less accurate results but do save more computing time. Also, small element size will increase the FE model's complexity which is only used when high accuracy is required. Large element size, however, will reduce the FE model's size and is extensively used in simplified models in order for providing a quick and rough estimation of designs. Due to its importance, in generating FEA models, the foremost problem is to choose appropriate elements size so that the created models will yield accurate FEA results while save as much computing time as possible.

The LDH simulation components and APA and GPG sandwich composite blanks were meshed using the Hypermesh tool. The four nodded rigid quadrilateral element (R-mesh) was used for the dome test tools – punch, binder and die, whereas the four nodded deformable quadrilateral element (Q-mesh) was used for the blanks. The Hypermesh tool automatically assigns the suitable element size for R-mesh. For the deformable body – blank – quad mesh (Q-mesh) type with element size of 1 mm is allotted. The mesh density is made very fine in order to emphasize the accuracy of the results.

3.8.3 LDH Simulation Process Parameters

The specified parameters include component geometries, element type, mesh density, punch travel speed, blank holding force and interface friction coefficient values. The Table 3.4 below indicates all parameters in detail.

Radioss Incremental Solver, which is one of the solvers in Altair Hyperworks software, is utilized to perform the LDH simulations. The input process parameters and geometrical specifications of the components – punch (dome shaped), binder, blank and die – are reproduced in the FEA software so as to simulate the experimental LDH test.

In LDH experiment, there is lock-bead mounted between die-flange and binder to hold the blank in place while the stretching takes place (as shown in Fig. 3.6). This lock-bead is imitated, on the FEA analysis, by a fixed edge constraint applied on the MPM sheet (as shown in Fig. 3.8) such that it can’t be drawn into the die cavity (pure stretching takes place).

The simulations are allowed to run until failure starts in the blank, and the dome height was taken just before failure. From the data obtained, forming limit diagram (FLD) and dome height graphs are plotted and analyzed thoroughly.

Table 3. 4: Process parameters

Parameters	Values
Punch travel speed (mm/min)	5000 & 10000
Punch dome diameter (mm)	101.6
Die cavity diameter (mm)	105.7
Die Cavity Fillet Radius (mm)	6.35
Blank dimensions	Indicated in Fig. 3.5
Blank element type and size (mm)	Q-mesh & 1
Interface Friction Coefficient (lubricated, dry)	(0.029, 0.42) for GPG & (0.04, 0.47) for APA
Binder – by keeping gap (mm)	1.5 for GPG & 2.5 for APA

The type of process used in the simulation is Double Action Draw. The setup window – with corresponding process parameters – is shown in Fig. 3.9. It is utilized to incorporate the process parameters – blank thickness and material properties, punch speed and binding mechanism. The obtained mechanical properties were fed into custom materials before they were assigned for the blanks. The friction conditions are applied under the 'Details' tab.

In order to incorporate the material properties into blanks in the Hyperworks simulation environment, Hill Orthotropic Tabulated material law was selected. Then, the respective yield strength, r-values, density, n-value and young's modulus were inserted. These materials are then added to the material database and applied for the blanks.

The MPM sandwich composite is replicated in the Hyperworks using ply laminate tool. The 'PCOMPP' material property is selected for the composite development. Then each layer is modelled as a ply with its respective thickness, material type and interface characteristics. These plies form a laminate which is the simulation counterpart of the MPM sandwich composite.

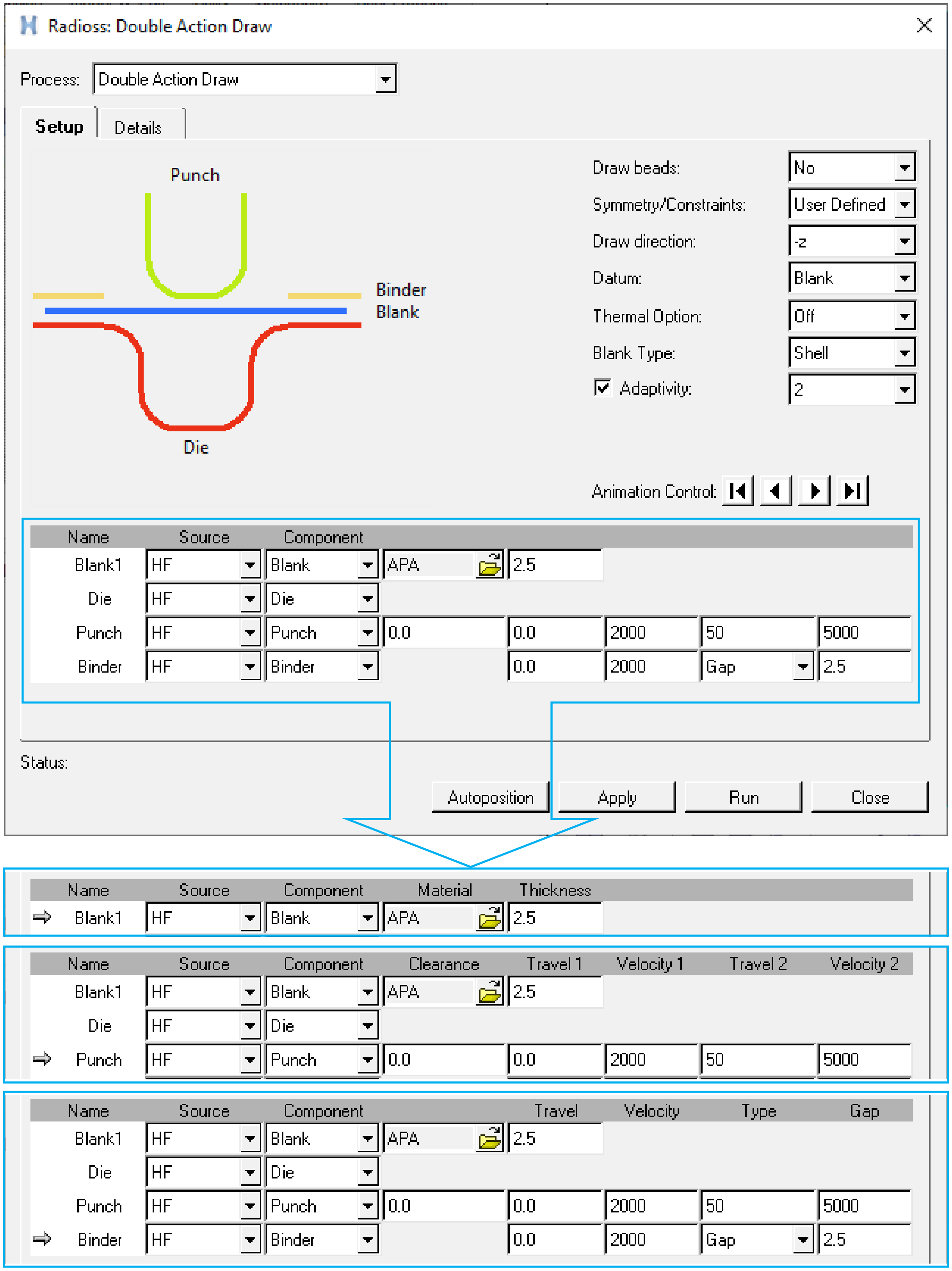

Figure 3. 9: Double Action Draw setup for APA sheet blank #1

3.9 Forming Limit Diagram (FLD)

The forming limit curve (FLC) is a failure limiting criterion for sheet metal forming. The entire diagram is known as a forming limit diagram (FLD). FLC illustrates the onset of localized necking in linear straining paths in a diagram of major and minor strains (i.e., in-plane minimum and maximum principal strains).

Forming Limit Curve (FLC), is a curve plotted between major strain and minor strain of the MPM sheet. Although a tensile test characterizes one specific strain path, a Forming Limit Curve (FLC) is necessary to have a map of strains indicating the onset of critical through-thickness necking for different linear strain paths. The strains which make up the FLC represent the limit of useful deformation. Calculations of safety margins are based on the FLC as shown in the simplified sketch below, Fig. 3.10.

Keeler and Brazier (1977) have proposed a relationship between lowest point on FLC (FLC_0) with strain hardening exponent (n) and sheet thickness (t), as indicated by equation (3.10). Keeler and Brazier equation is valid for a given range of n and t; n ≤ 0.21, t ≤ 3.1.

$$FLC_0 = ln\left[1 + \left(\frac{23.3+14.13t}{100}\right)\frac{n}{0.21}\right] \quad (3.10)$$

The FLC's left side has followed a straight line with a slope of '–1', as shown in equation (3.11) below.

$$\varepsilon_1 = FLC_0 - \varepsilon_2 \quad (3.11)$$

Other researchers also used the same equation to predict the FLC's left side (B.S. Levy, and C.J. Van Tyne, 2016). equation (3.12) is used to calculate the FLC's right side.

$$\varepsilon_1 = (1 + FLC_0)(1 + \varepsilon_2)^{0.5} - 1 \quad (3.12)$$

According to (Surajit Kumar Paul, 2021), equation (3.11) is utilized to calculate the FLC's left side. equation (3.13) is used to compute the right side of the FLC. The present thesis work also applies these equations because of their comprehensive approach.

$$\varepsilon_1 = (1 + FLC_0)(1 + \varepsilon_2)^{p} - 1 \quad (3.13)$$

Where exponent "p" is a material constant, and it can be calculated using equation (3.14).

$$p = 1.0834Exp(-1.4114FLC_0) - 0.361 \quad (3.14)$$

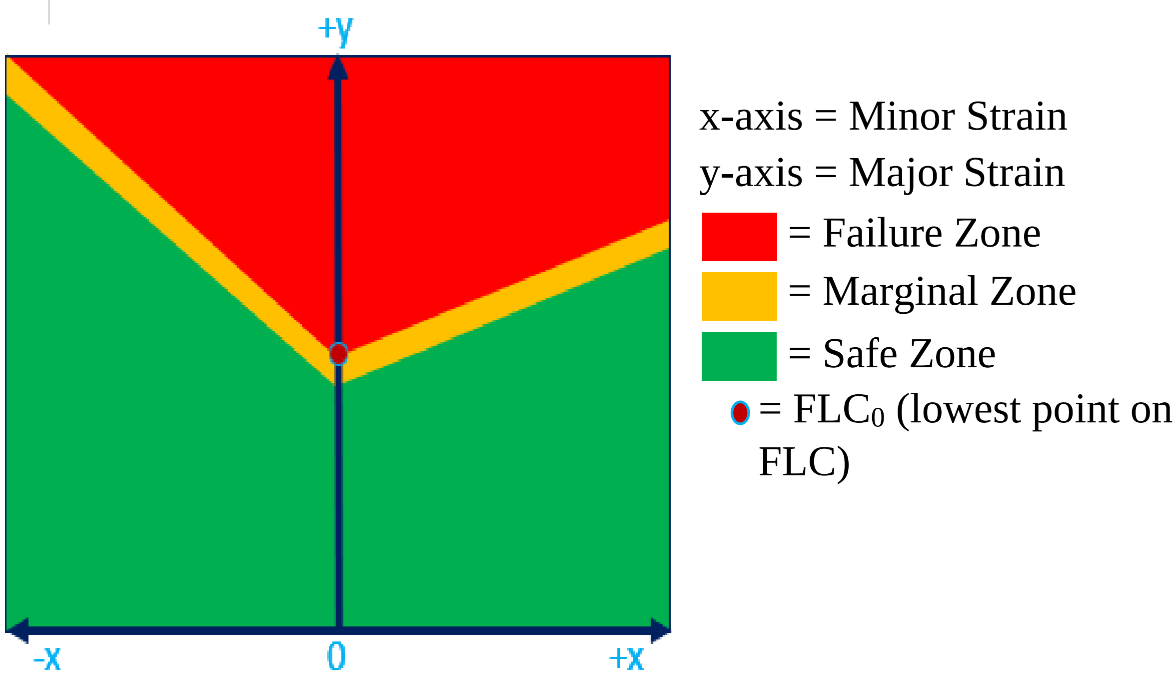

Figure 3. 10: Simplified Schematic FLD

Etching a blank of MPM sheet with circular grids helps visualize strain paths. After forming, the circles turn into ellipses as shown in Fig. 3.11, with the dimensions of major and minor axes related to the major and minor strains respectively. Figure 3.11 depicts the deformation of a circle of the grid into elliptical forms. The major strain is defined as the greatest strain, while the minor strain is defined as the least strain at that particular location. The oval on the right represents the case where both the major and minor strains are positive. The oval on the left represents the case where the major strain is positive while the minor strain is negative. This forms the basis for Circle Grid Strain Analysis (CGSA).

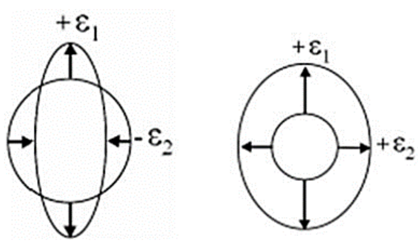

Figure 3. 11: Minor and Major Deformation Diagram

There are two sub-branches of FLC, ‘‘right branch’’ for positive minor strain (i.e., stretching), while the ‘‘left branch’’ for negative minor strain (i.e., drawing), which can be illustrated in detail in the following Fig. 3.12 (Surajit Kumar Paul, 2021).

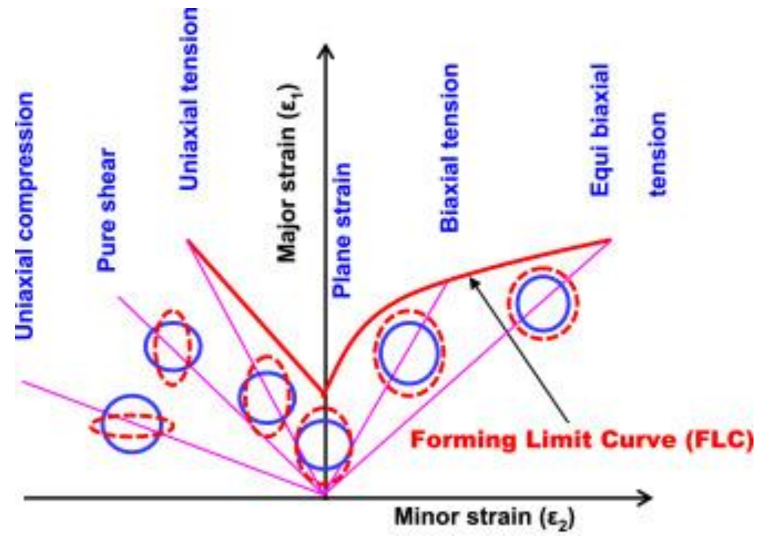

Figure 3. 12: Detailed representation of FLD *(Surajit Kumar Paul, 2021)*

The major and minor engineering strains (e_1 and e_2) can be calculated by using equation (3.15). equation (3.16) is used to calculate the major and minor true strains.

$$e_{1,2} = \frac{d_{1,2} - d_0}{d_0} \quad \text{.......(3.15)}$$

$$\varepsilon_{1,2} = \ln(1 + e_{1,2}) \quad \text{.......(3.16)}$$

Where: e_1=engineering major strain d_0=circular grid original diameter

e_2=engineering minor strain d_1=major axis diameter

ε_1=true major strain d_2=minor axis diameter

ε_2=true minor strain

According to (Surajit Kumar Paul, 2021), equation (3.16) is valid up to the necking initiation.

FLD curves can also be obtained when MPM sheet is deformed by In-Plane Stretching of flat specimens in free space. In this kind of test there is no specimen curvature, no strain gradients, and no interface friction present. Compared to out of plane stretching tests (like dome tests), in-plane forming limits can be more sensitive to material defects and are not influenced to the same extent by tooling geometry variables (K.S. Raghavan, 1995). Furthermore, since curvature and friction effects are absent, large strain gradients can be avoided in the in-plane test, allowing forming limits to be more accurately defined. Despite these advantages, the in-plane approach is not widely used to develop forming limit curves, perhaps because of the lack of a good streamlined technique to determine forming limits in different strain paths. These tensile deformation methods are capable of producing strain paths only on the left-hand side of the FLD, ranging from uniaxial tension to plane strain.

The strain gradient is the rate at which strain changes through a part. Since this plane-strain tensile test specimen is in pure tension, it will have no strain gradient because the whole specimen is at the same strain. In dome stretching tests (having multiple strain paths) however, some portion of the specimen will be under tension and the rest under compression. The rate at which strain changes throughout the cross-section of the specimen is its strain gradient.

Geometries for plane-strain tensile test specimens are selected based on Leo Joseph Kilfoil (2007). The schematic representation of these specimens is indicated in Fig. 3.13 below. The flat MPM sheet specimen has length and width. Hence, when strains are imposed through plane-strain tensile tests on samples that are shown in Fig. 3.14 and 3.15, FLC can be generated in the plane strain direction.

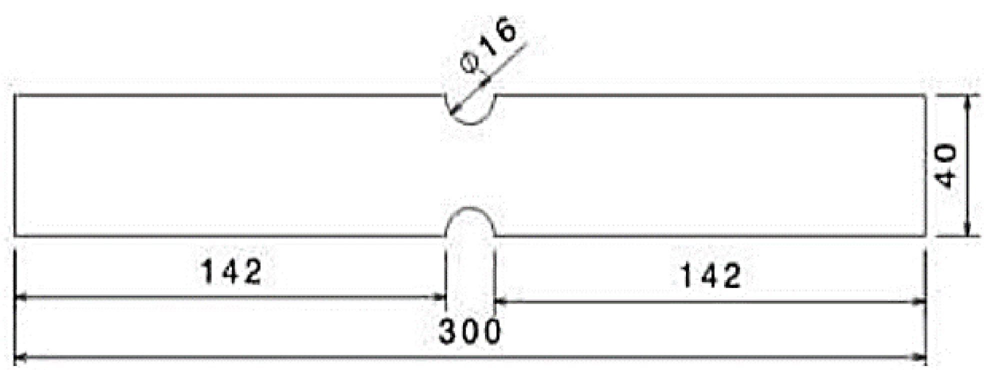

Figure 3. 13: Schematic of plane-strain tensile test specimen [Dimensions in mm] ***(Leo Joseph Kilfoil, 2007)***

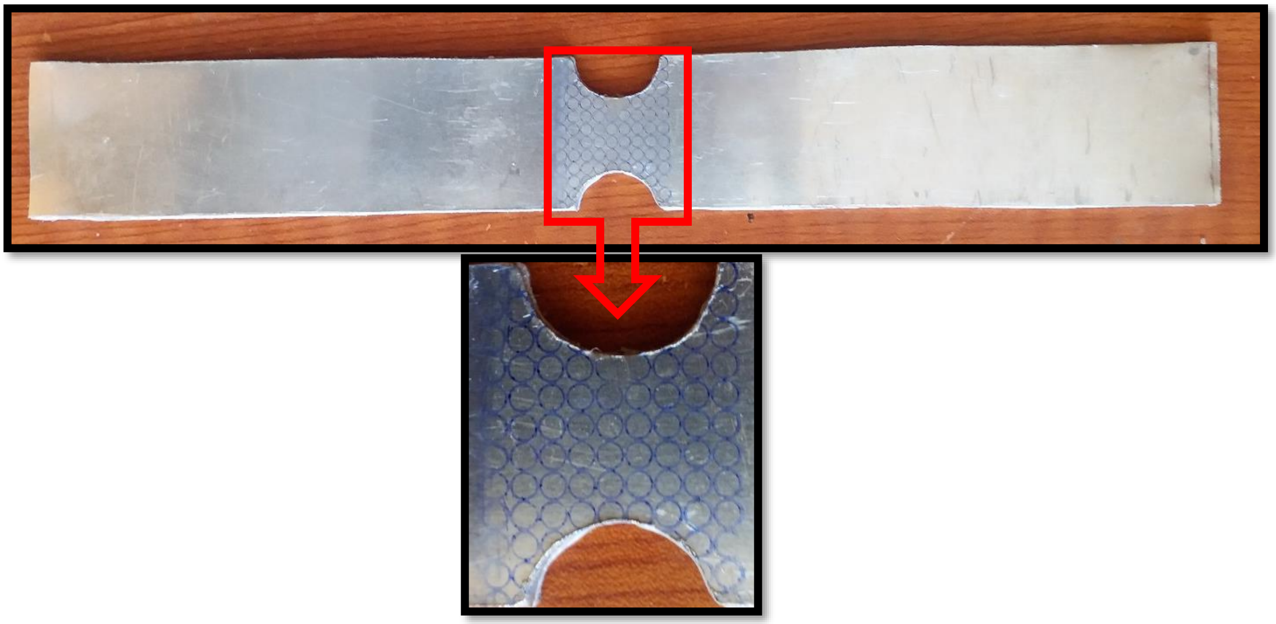

Figure 3. 14: APA specimen for plane-strain tensile test

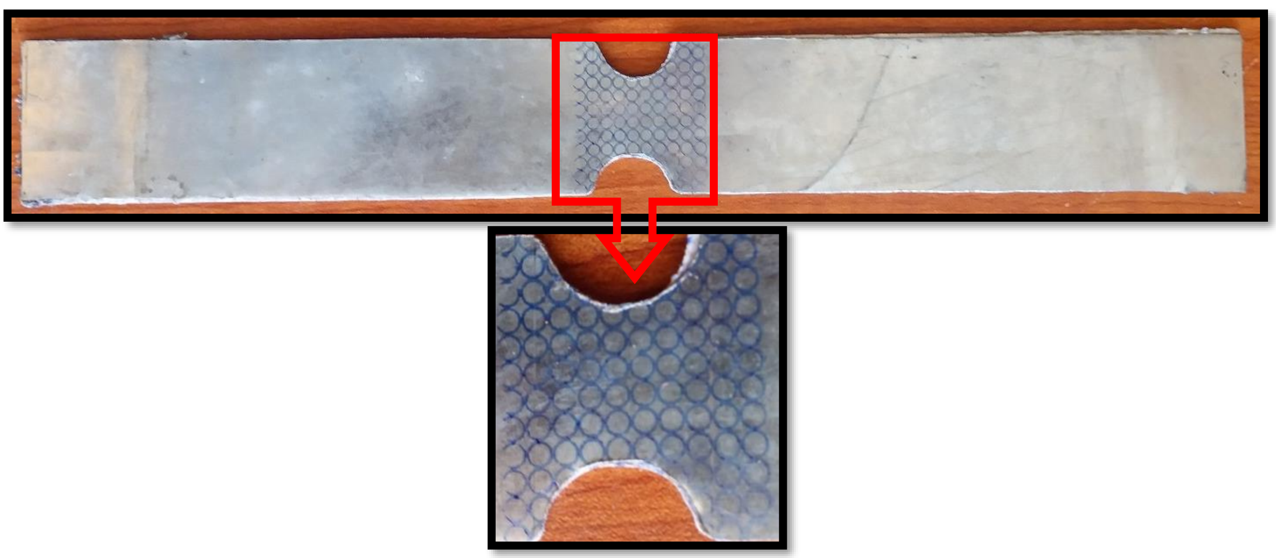

Figure 3. 15: GPG specimen for plane-strain tensile test

The FLD strain (for In-Plane Stretching) can be readily obtained by measuring the strain level at a location removed from the fracture site. Since no strain gradient exists prior to the onset of necking, and since no increase in the strain plateau occurs during the development of the neck and fracture, the strain state at a location removed from the fracture site is identical to that which exists at the fracture site at the onset of localized necking (S. P. Keeler, 1978).For multiple strain path forming experiments, (Surajit Kumar Paul, 2021), a very comprehensive Forming Limit Diagram (FLD) can be generated as shown in the Fig. 3.16 below.

This curve indicates the maximum strain that the material can withstand prior to necking (or in sheets – extreme thinning). With these limit values, forming operations will be carefully designed under the permissible strain range. The FEM simulation counterpart of this study is the LDH simulation – undertaken via Altair Hyperworks tool. In addition to FLC, maximum dome height (before thinning/necking) is extracted from the LDH simulation.

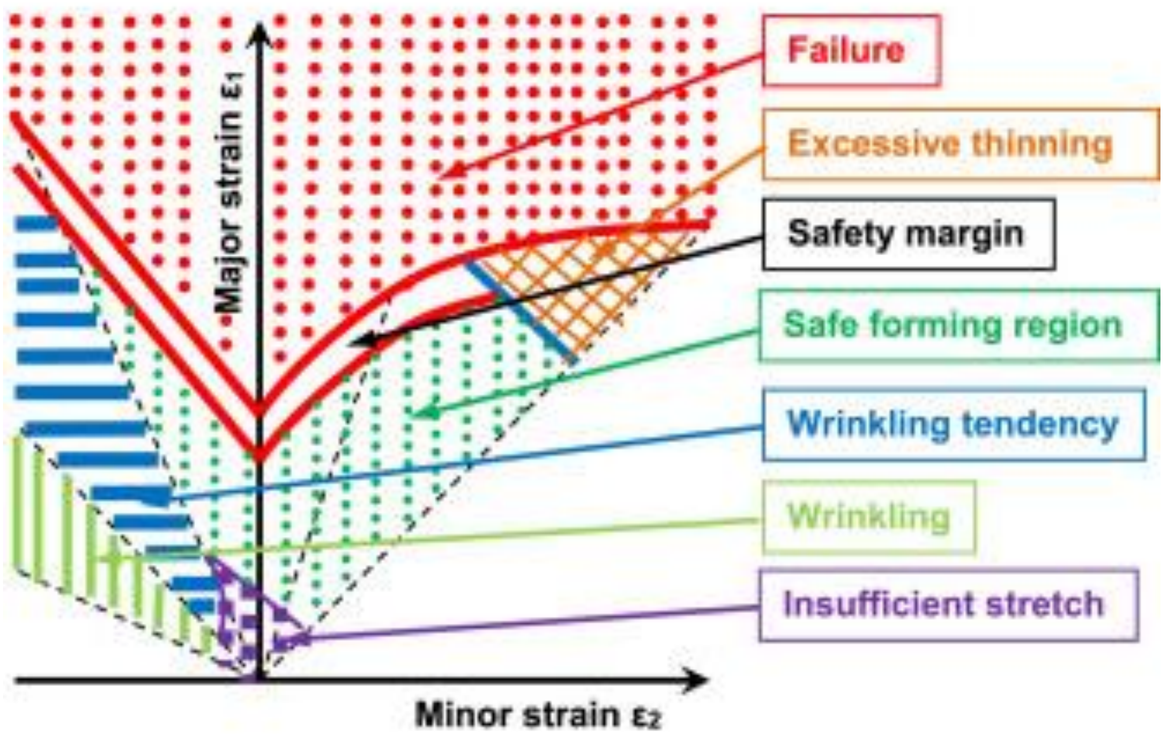

Figure 3. 16: Zones in FLD *(Surajit Kumar Paul, 2021)*

3.10 Adhesive test

Taking the performance of the adhesive utilized in the MPM composite under consideration is one of the focus points of this study. In order to accomplish that, lap-joint adhesive tests are executed. Single-lap adhesive test is performed on a sample made of the adherends that overlap with the adhesive applied in between as per the ASTM D5868 Standard specifications, as shown in Fig. 3.17.

These adherends (aluminum, galvanized steel and PVC sheets) have passed through the same preparation process as the MPM composites, so that these test results could indicate the MPM laminate composite's integrity. The samples for this test are indicated in Fig. 3.18.

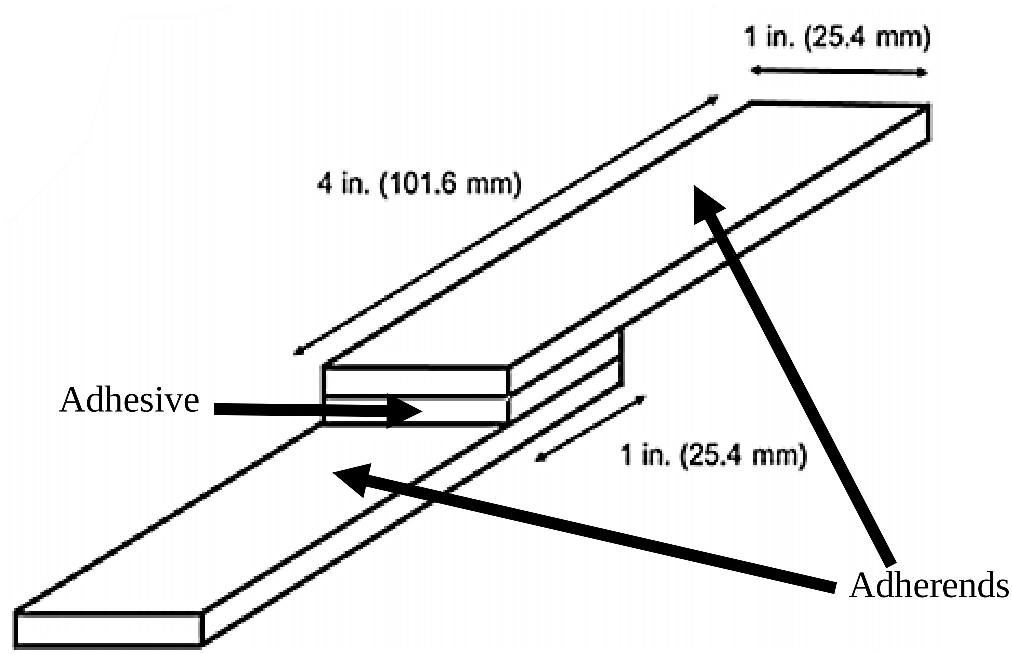

Figure 3. 17: Single-lap adhesive test sample *(ASTM D5868)*

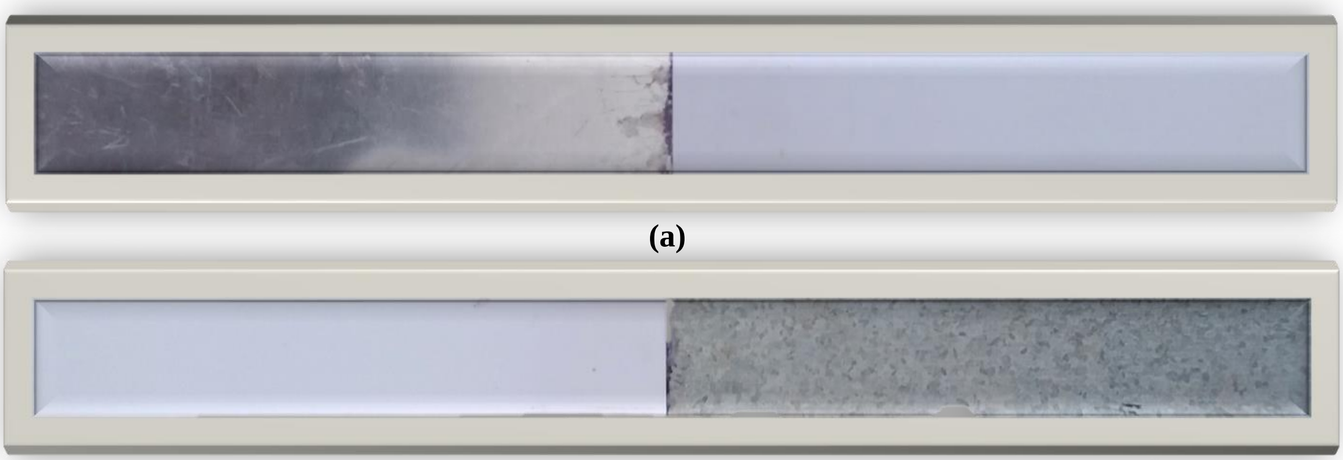

(a)

(b)

Figure 3. 18: Aluminum with PVC (a), Galvanized steel with PVC (b)

3.11 Density

One of the main reasons for the necessity of this MPM sandwich composite is its light weight characteristics. This is illustrated as, for sheets of similar dimensions (and hence similar volume) – one of them being monolithic metallic sheet and the other MPM sandwich composite – their weight will be different due to density variances. The relatively low density of the included polymer is responsible for this weight reduction. Table 3.5 indicates the densities of the constituent materials.

Table 3. 5: Densities of the constituent materials

Material	Density (g/cm^3)
Aluminum	2.7
Galvanized steel	7.874
PVC	1.38
Epoxy	1.2

In order to analyze to what extent this weight reduction is attained, the densities of both MPM sandwich composites have been calculated.

The simple mass density of composite materials, or materials made from two or more distinct materials with known individual densities, can be worked out using a simple process.

Step 1: Find the densities of all the constituent materials.

Step 2: Convert each constituent's percentile contribution to the mixture to a decimal number (a number between 0 and 1) by dividing by 100.

Step 3: Multiply each decimal by the density of its corresponding constituent material.

Step 4: Add together the products from step 3. This will be the density of the sandwich composite in the same units selected at the start or the problem.

CHAPTER 4
Results and Discussion

4.1 Introduction

The results obtained from experimentation – tensile test, in-plane stretching, plastic strain (r-value) determination, single lap adhesive test and weight reduction evaluation – and from LDH simulation are discussed in detail in this chapter.

4.2 Tensile Properties

Tension tests, which have been undertaken on a Universal Testing Machine (UTM) at room temperature, revealed the mechanical properties of the materials. First, the base materials, which constitute the MPM laminate composites (aluminum, galvanized steel and PVC sheets) are tested in order to determine their ultimate tensile strength (UTS), yield strength (σ), total and uniform elongation, strength coefficient (K) and strain hardening exponent (n) values. For the metallic sheets, the tests are performed in three rolling directions (0^0, 45^0, 90^0) to take into account the effects of anisotropy. Figures 4.1, 4.2 and 4.3 below show the tensile test samples (as per ISO 6892-1 specification) for base materials – before and after rupture.

(a) (b)

Figure 4. 1: GSS tensile test (90^0 orientation) – before rupture (a), after rupture (b)

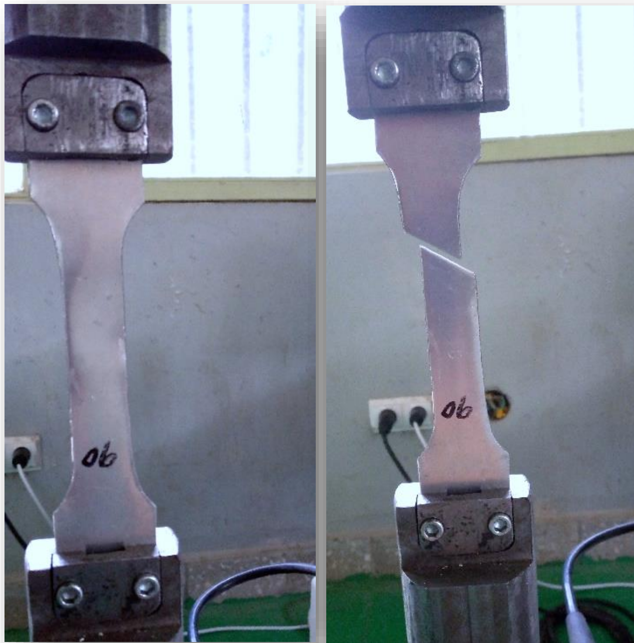

(a) (b)

Figure 4. 2: Al-sheet tensile test (90^0 orientation) – before rupture (a), after rupture (b)

(a) (b)

Figure 4. 3: PVC-sheet – before rupture (a), after rupture (b)

Once the mechanical properties of the constituent materials have been studied, the same procedure is applied for MPM sandwich composites – made from aluminum with PVC and galvanized steel with PVC – in order to determine the aforementioned properties. Metallic sheets of similar rolling direction are used to make each sample. Since PVC is isotropic, it doesn't have directionality. PVC have shown a ductile failure phenomena since it has plastically deformed and necked before rupture. The samples prepared for this test – before and after rupture – are shown in Fig. 4.4 and 4.5 below.

(a)

(b)

Figure 4. 4: Tensile test specimens – APA (a), GPG (b)– before deformation

(a)

(b)

Figure 4. 5: MPM tensile tests – APA (a). GPG (b)– after rupture

4.3 Stress and Strain

From the force and elongation data obtained from the tensile tests, engineering stress, engineering strain, true stress and true strain are calculated using equations 3.1, 3.2, 3.3, and 3.4 respectively. These values are also studied in three rolling directions (0^0, 45^0, 90^0), so that anisotropic directionality effects are taken into consideration.

From stress-strain plots – shown in Fig. 4.6, 4.7, 4.8 and 4.9 – yield strength, Ultimate Tensile Strength (UTS), maximum allowable elongation before necking and before rupture are studied.

Further analysis provided the K and n values. All of these results are tabulated in Table 4.1 shown below.

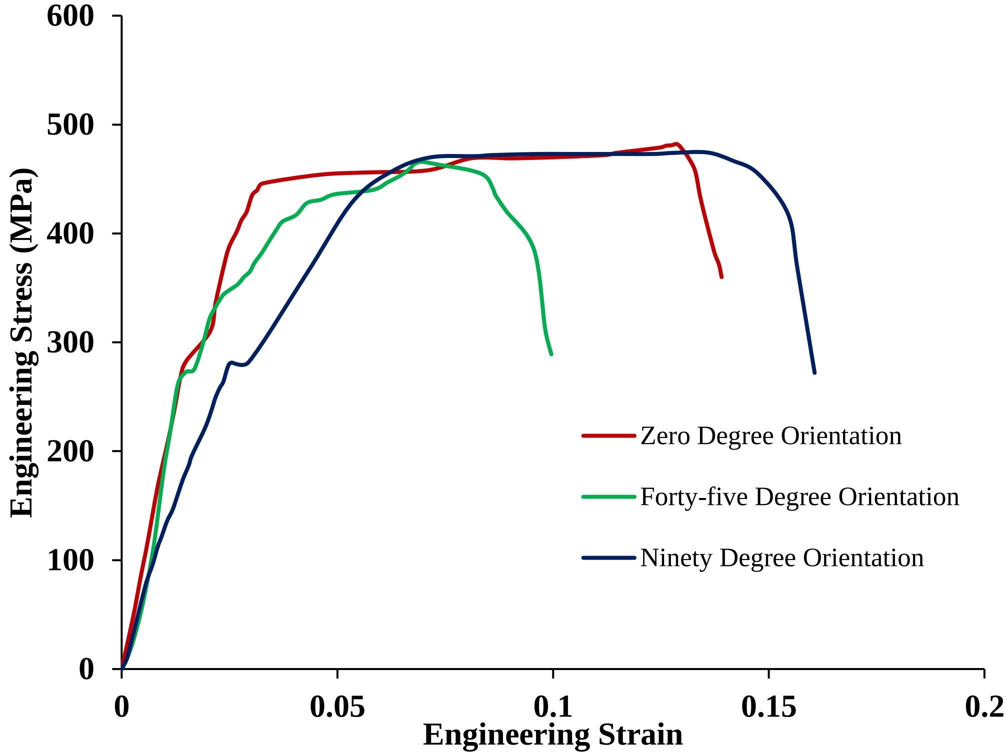

Figure 4. 6: Engineering Stress-Strain of GSS

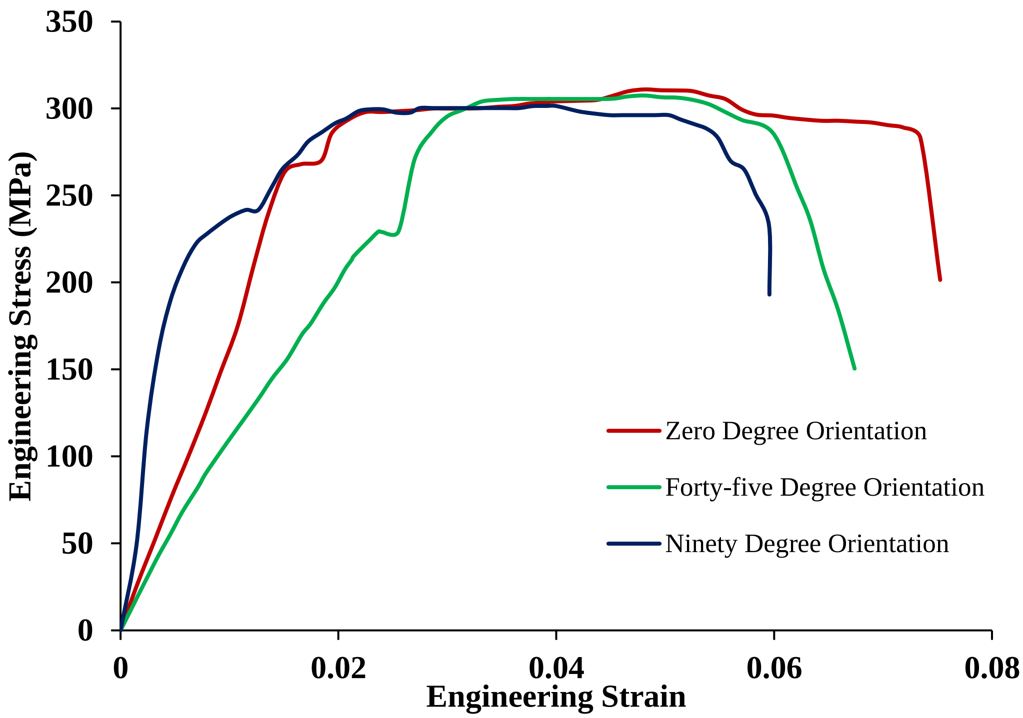

Figure 4. 7: Engineering Stress-Strain of Al-sheet

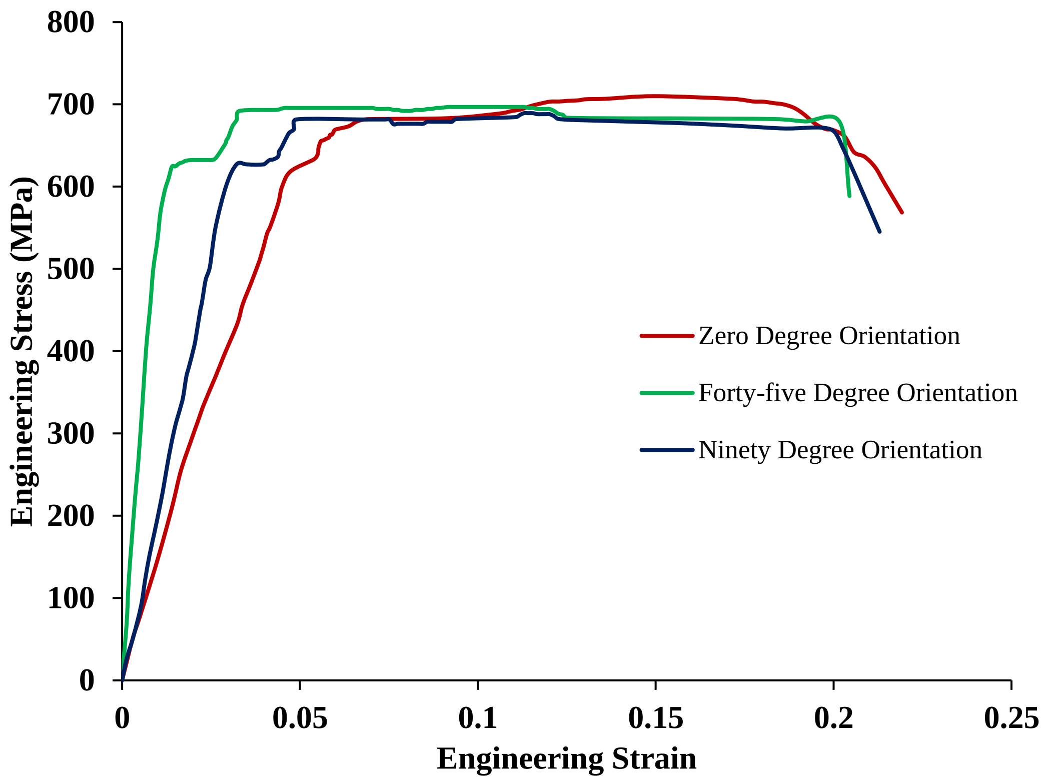

Figure 4. 8: Engineering Stress-Strain of GPG

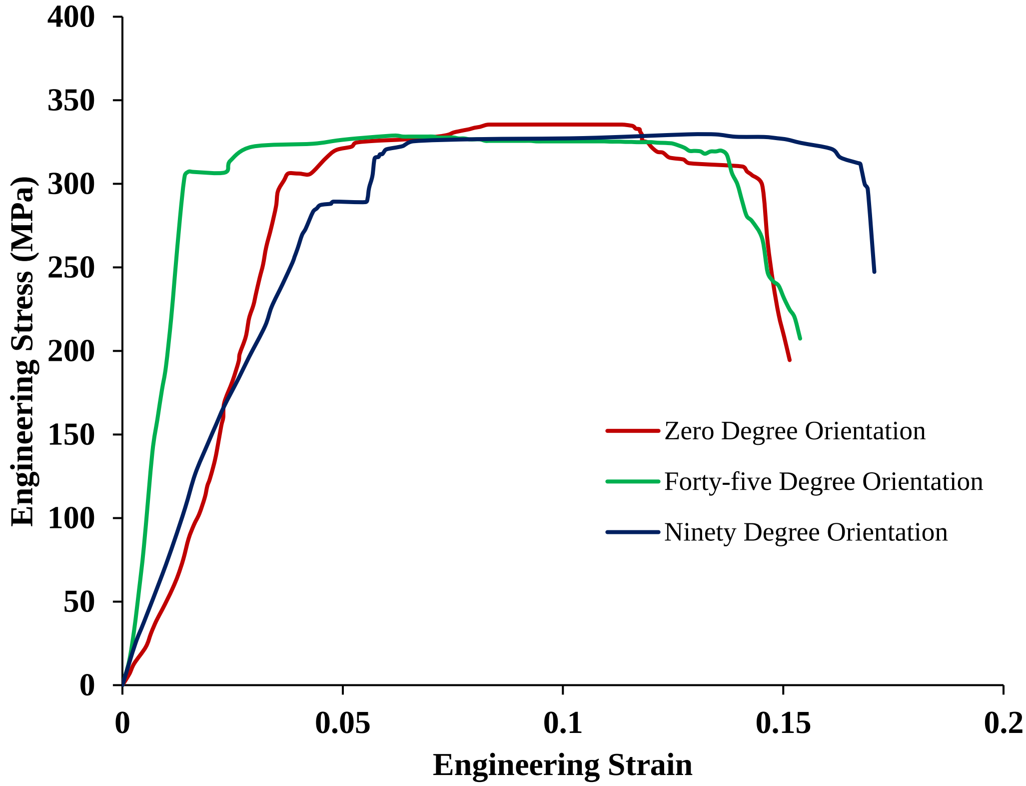

Figure 4. 9: Engineering Stress-Strain of APA

Table 4. 1: Mechanical properties of base and composite materials

Materials	Yield strength (MPa)	UTS (MPa)	Strength coefficient, K (MPa)	Hardening exponent, n	Plastic strain ratio, r	Total elongation	Uniform elongation
Al-sheet	260.49 ± 8.46	308.60 ± 11.62	423.0013 ± 13.69	0.27 ± 0.03	0.8869 ± 0.09	4.8127 ± 1.06	3.3526 ± 0.74
GSS	287.77 ± 9.38	474.56 ± 9.75	555.0930 ± 16.37	0.22 ± 0.04	1.6101 ± 0.11	8.7023 ± 1.49	6.7479 ± 0.98
PVC	-	78.5 ± 2.81	-	-	-	46.7098 ± 3.42	37.2469 ± 3.07
GPG	648.13 ± 14.54	701.57 ± 10.82	958.04 ± 20.458	0.2 ± 0.02	1.6455 ± 0.18	17.2724 ± 2.18	9.5017 ± 1.97
APA	314.43 ± 9.74	333.66 ± 8.42	475.1 ± 15.776	0.25 ± 0.05	1.1192 ± 0.26	12.5861 ± 1.93	8.6875 ± 2.04

We cannot make comparison between both types of MPM sandwich composites and their respective base material (in terms of yield strength, UTS and total elongation) since the evaluated materials are of different thicknesses and testing took place at different strain rates. Instead, their hardening exponent (n) have shown comparable value to their constituent metallic sheets.

As Table 4.1 and engineering stress-strain diagram of GSS indicate (as shown in Fig. 4.6), the material behaves more or less similarly in the three orientations to the rolling direction – 0, 45 and 90 degrees. However, engineering stress-strain diagram of Al-sheet (as shown in Fig. 4.7) clearly shows that it is slightly anisotropic since the obtained values in the three orientations indicate discrepancies.

Since these metallic sheets are members in the MPM sandwich composites – APA and GPG – their anisotropic effect is also observed in the composite laminates (as shown in Table 4.1, Fig. 4.8 and 4.9). Hence, APA has more anisotropic behavior compared to GPG.

4.4 Strain Hardening

The MPM sandwich composites contain metallic elements as constituent components. Since these metallic components – Al-sheet and GSS – are susceptible to work hardening (strain hardening), the MPM sandwich composites – APA and GPG – will also undergo strain hardening.

Equation 3.5 can be used to determine the relationship between true stress and true strain while strain hardening phenomenon of these materials take place. The strain hardening exponent (n) and the strength coefficient (K) values are extrapolated from stress-strain graphs as indicated in Table 4.1.

The n-value of base materials and the corresponding composites are found to be comparable. This indicates that their deformation mechanism is more or less analogous.

4.4 Plastic Strain Ratio (r-value)

Equation 3.7 is used to calculate the plastic strain ratio (r) manually by measuring the change in axial gage length and the change in width. In this manual approach, prior to testing the specimen (as shown in Fig. 4.10) width and distance between gage marks is measured with calipers. Figure 4.11 shows the test procedure. The specimen is then pulled to a strain less than at maximum force (before onset of necking) – 10 % elongation – and then unloaded. The final width and gage length are then measured to determine r-value.

The obtained values are indicated in Table 4.1 above. Using the r-values in the three directions (0^0, 45^0, and 90^0 to the rolling direction), two other important parameters – Planar anisotropy parameter (Δr) and Normal anisotropy parameter (r_m) – are calculated using equation (3.8) and (3.9) respectively. Planar anisotropy parameter (Δr) is an indicator of the ability of a material to demonstrate a non-earing behavior and it is preferred to be as small as possible. On the other hand, Normal anisotropy parameter (r_m) is an indicator of the ability of a material to be deep drawn and it is preferred to be as high as possible. Table 4.2 shows these values for base and MPM composite materials.

Figure 4. 10: Testing procedure – base material (Al-sheet)

Table 4. 2: Planar anisotropy parameter (Δr) and Normal anisotropy parameter (r_m) values

Material	Planar anisotropy parameter (Δr)	Normal anisotropy parameter (r_m)
Al-sheet	0.02726	0.89147
GSS	0.22167	1.57416
APA	0.25353	1.07696
GPG	0.25333	1.60333

From the results tabulated in Table 4.2, it can be observed that Al-sheet has better non-earing behavior compared to GSS, whereas, APA and GPG have comparable values. On the other hand, GPG ranks the highest value for deep-drawability. The rest – GSS, APA, Al-sheet – follows GPG in descending order.

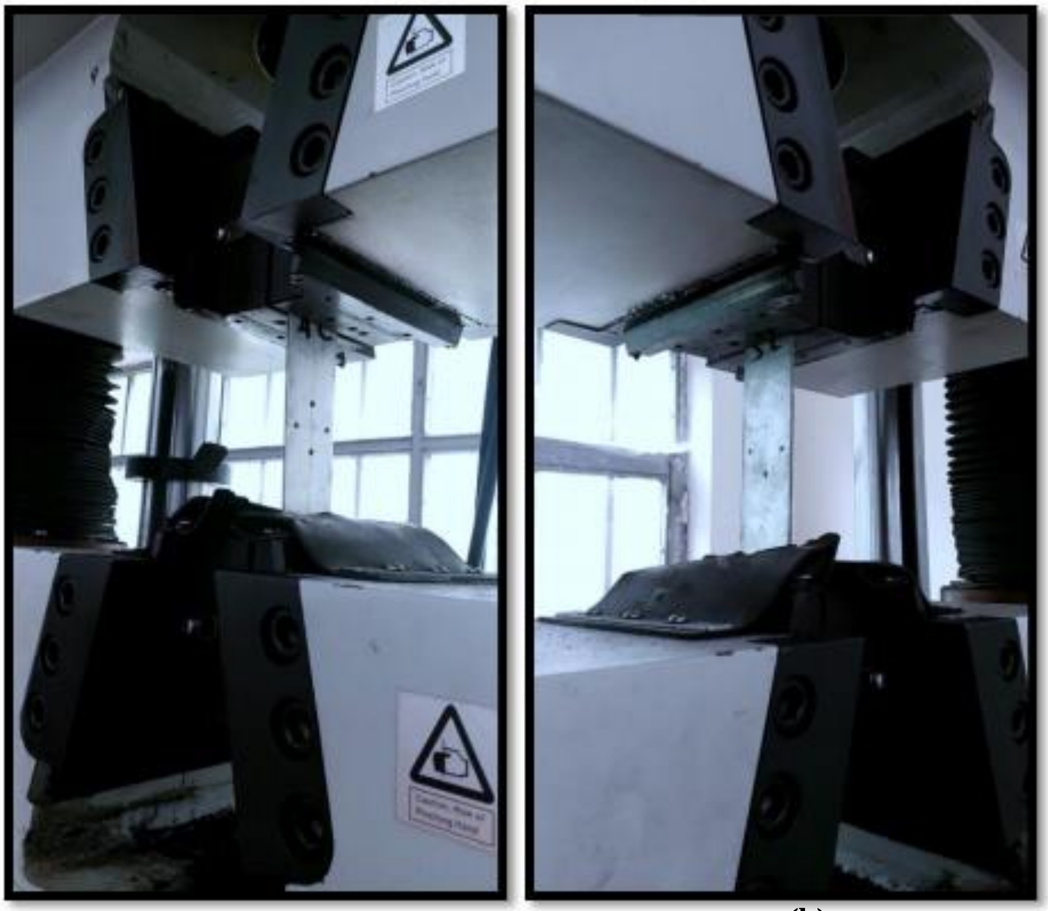

(a) (b)

Figure 4. 11: r-value test procedure – APA (a), GPG (b)

4.5 Adhesive Strength

Single-lap adhesive test is performed (as shown in Fig. 4.12) on samples made of the adherends – Al-sheet with PVC and GSS with PVC – that overlap with the epoxy adhesive applied at their interfaces. In both cases, the PVC adherend ruptures before the adhesion fails, as shown in Fig. 4.13 below.

(a) **(b)**

Figure 4. 12: Single-lap adhesive test procedure – GSS with PVC (a), Al-sheet with PVC (b)

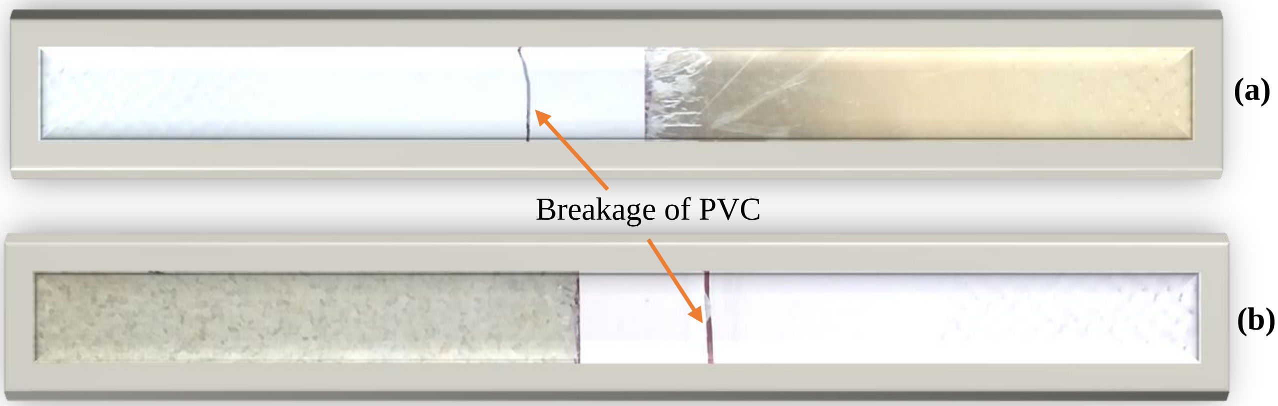

Figure 4. 13: Adhesive test samples after rupture – Al with PVC (a), GSS with PVC (b)

The fact that one of the adherends (PVC) ruptures before the adhesive at the interface fails (or the bond breaks) is a good result. It means that the bond created via the epoxy adhesive can withstand load until one of the substrate materials breaks or ruptures.

Even though these test results indicate enough bond being created in both metal-polymer adherends, when comparison is made (during other mechanical tests) between the two MPM composites – APA and GPG – the former reveals better adhesion and bonding strength than the later. This is due to the fact that GSS has high abrasion resistance. The epoxy adhesive creates the bond by entering into the asperities of adherend surfaces and curing in between them – as a result, forming mechanical interlocking. Since GSS cannot be easily abraded – to form micro-grooves and asperities – not adequate mechanical interlocking takes place, and hence weaker bond. Al-sheet and PVC, on the other hand, can be abraded without difficulty, and create a stronger mechanical interlocking and bond.

For the GPG composite, better adhesion can be achieved through other MPM manufacturing methods (hand layup method is used for this research), like warm roll bonding (WRB), in which the substrate materials are pre-heated for better adhesion and stronger bond.

4.6 Limiting Dome Height (LDH) Simulations

LDH simulations with various combinations of geometry and process parameters are performed using the Hyperworks software. The properties of the APA and GPG sandwich sheets that have been obtained through empirical testing are replicated with FE models in Hyperworks and simulations are conducted using Radioss-Incremental solver. The average simulation time for all the simulations is 58 minutes.

FE simulations for the LDH test indicate that the test is very sensitive to friction and it affect the test measurements. Friction at tool-workpiece interface (in this case, mainly at punch-blank interface) has an effect on formability and thinning distribution. It can be expected that maximum thinning when friction is zero occurs at the apex of the dome. Some simulations have been conducted with zero interface frictional value (between punch and blank), and the failure did in fact occur at the tip of the dome. Figure 4.14 indicates this condition for APA blank #1. Generally, location of maximum thinning moves away from the apex of the dome (moves toward die corner radius) as interface friction increases, and punch force also increases as interface friction increases.

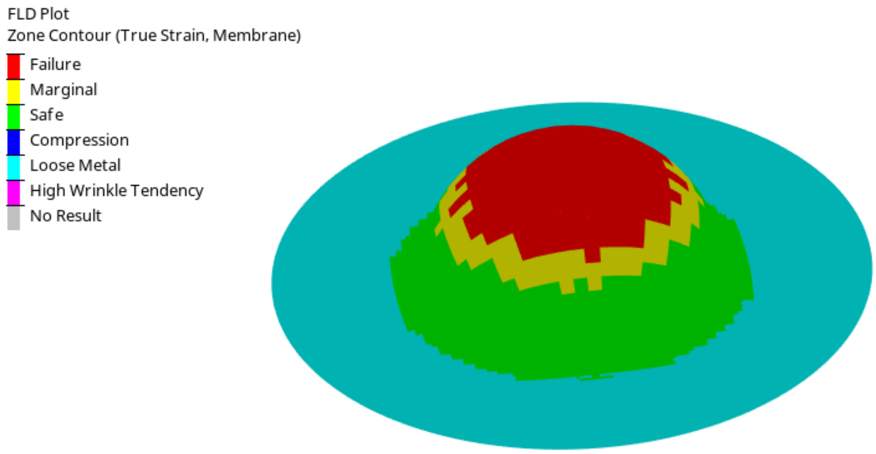

(a)

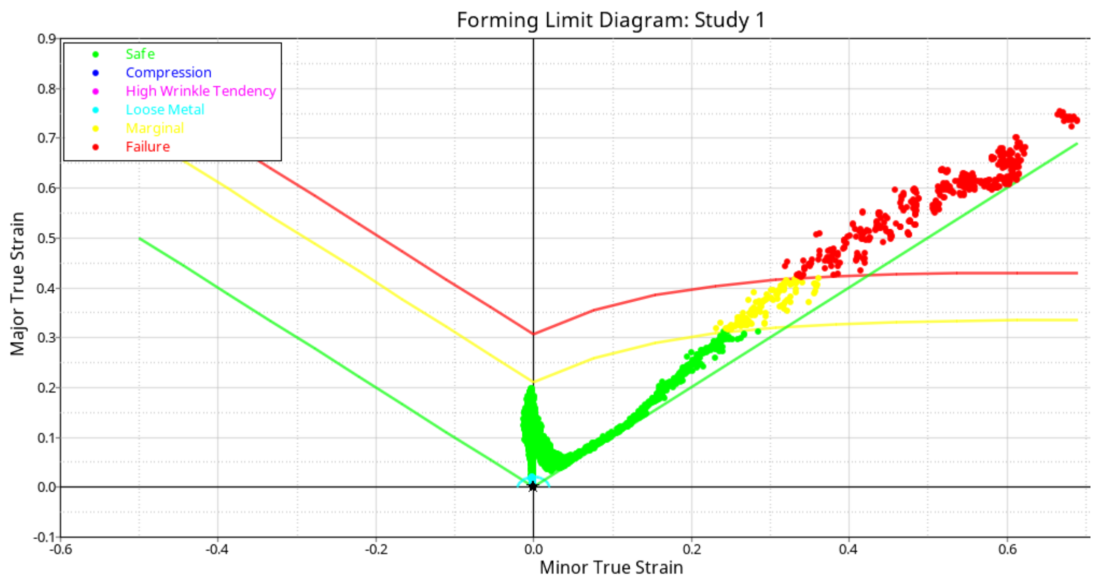

(b)

Figure 4. 14: APA blank #1 with zero friction coefficient between punch and blank – Deformed blank (a), FLD (b)

From Fig. 4.15, it clear that failure zones are in the side wall of sandwich dome, which means more thinning has happened in the side wall of sandwich sheet along with punch travel. From all the simulations in the bi-axial sandwich sheets, almost similar failure phenomenon is noticed.

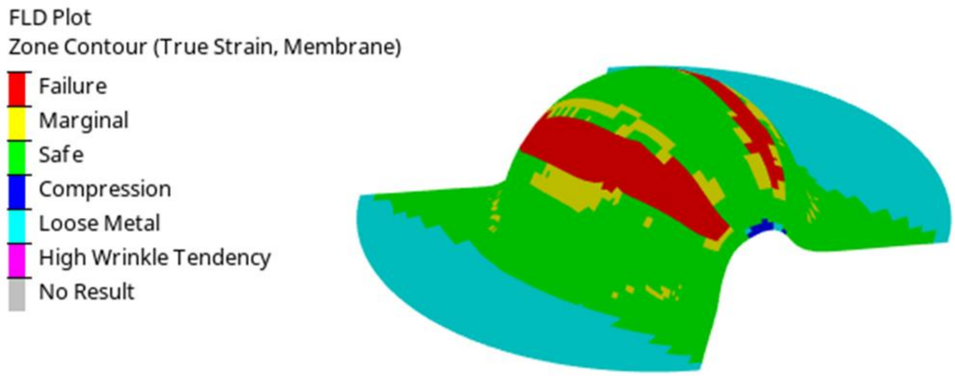

(a)

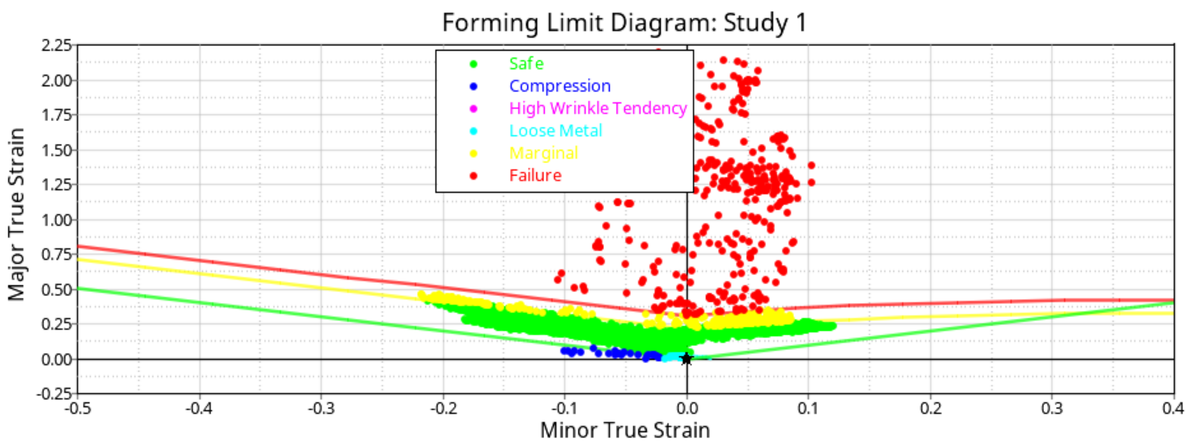

(b)

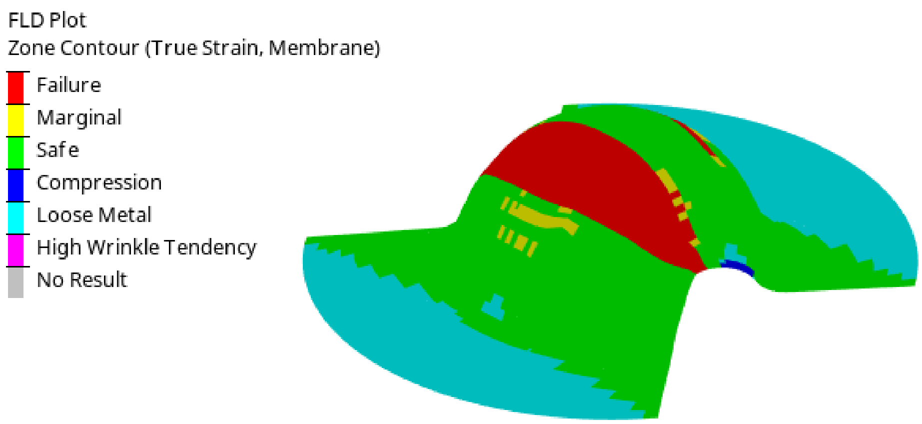

(c)

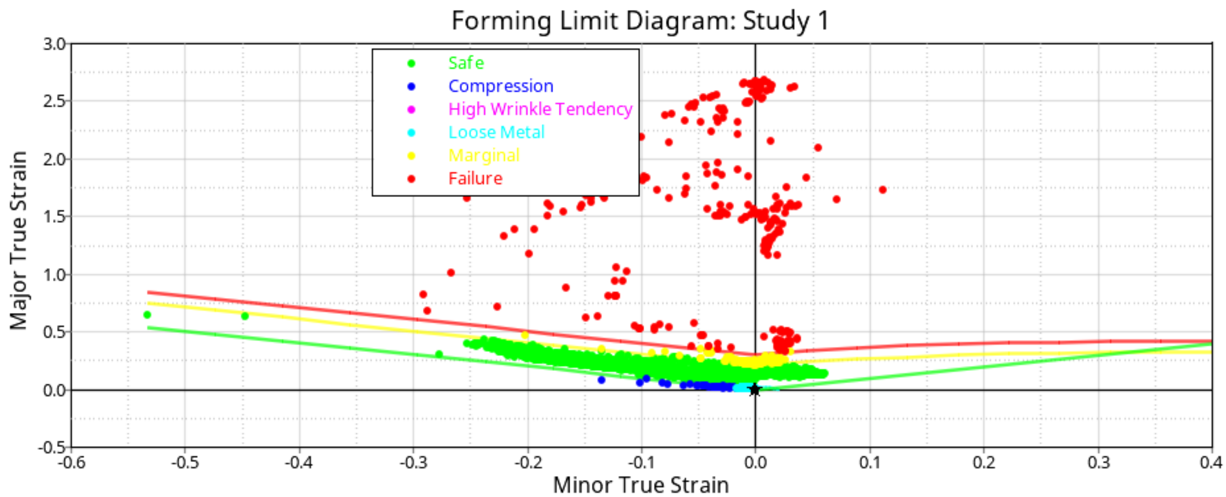

(d)

Figure 4. 15: Contour plot and FLD of: APA blank #6 - (a) and (b), GPG blank #6 - (c) and (d)

4.7 Forming Limit Diagram (FLD)

Forming limit diagrams (FLDs) which encompass forming limit curves (FLCs) have been generated from plane-strain experimentations – single strain path – and from simulations – multiple strain path. The FLC is a failure limiting criterion for sheet material forming. The entire diagram is known as FLD – which indicates thinning, wrinkling tendency, insufficient stretch and safe forming zones in addition to FLC. FLC illustrates the onset of localized necking in linear straining paths in a diagram of major and minor strains (i.e., in-plane minimum and maximum principal strains). The test samples – with circular grid markings – have been stretched till failure (as shown in Fig. 4.16), and the ellipses' major and minor diameters are measured. The lowest point on FLC (FLC_0) is then calculated – using equation 3.10 – to be 0.3283 for APA and 0.6043 for GPG. These values are comparable with those obtained from the simulations (as shown in Fig. 4.17). The major and minor engineering strains (e_1 and e_2) are calculated by using equation (3.15) and equation (3.16) is used to calculate the major and minor true strains (ε_1 and ε_2). Table 4.3 indicates these values.

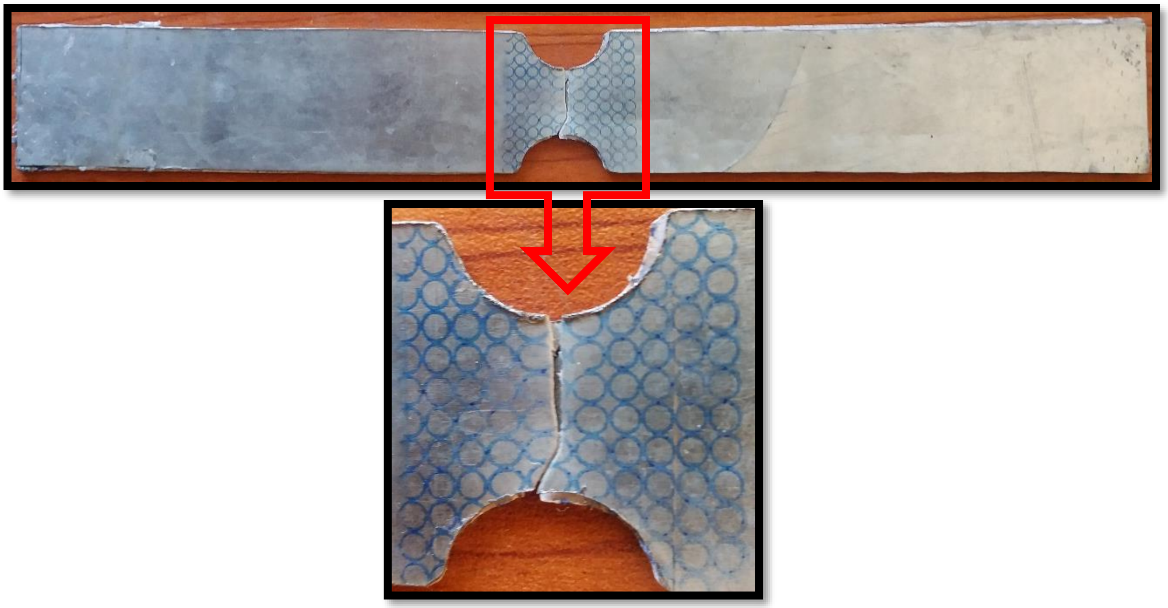

(a)

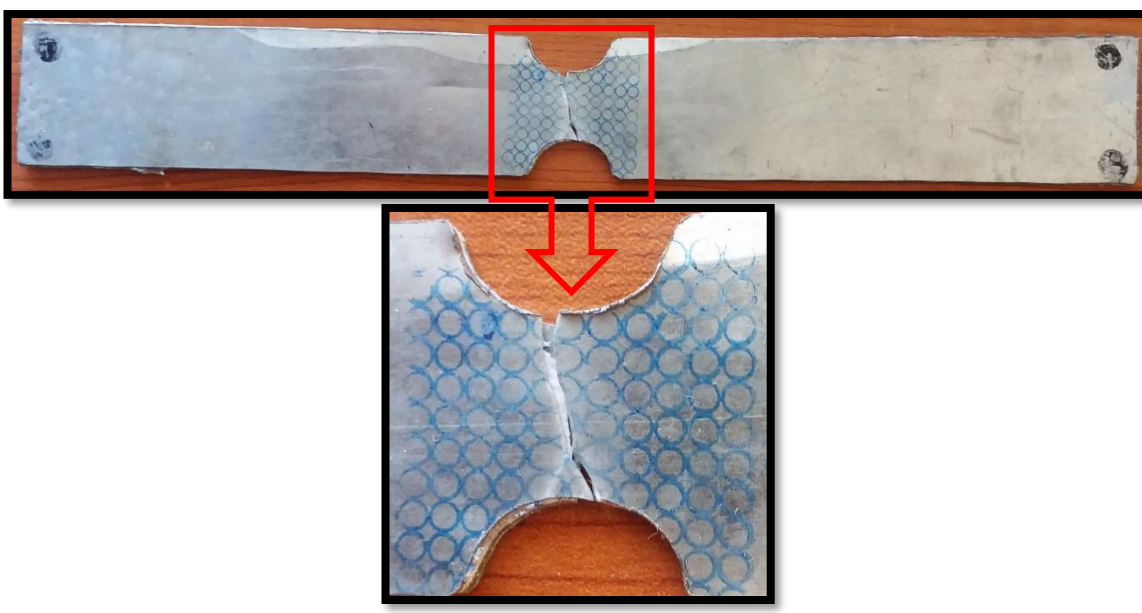

(b)

Figure 4. 16: Plane-strain test samples after rupture and ellipse formation – APA (a), GPG (b)

Table 4. 3: Calculated values of e_1, e_2, ε_1 and ε_2

Material	e_1	e_2	ε_1	ε_2
APA	0.4167	0.33	0.3283	0.2876
GPG	0.83	0.67	0.6043	0.5128

The average forming limit curve (FLC) – obtained from simulations – for both APA and GPG sandwich sheets are shown in Fig. 4.17 and Fig. 4.18. The comparison of FLC_0 values obtained from experiment and simulation revealed standard error of 5.6 % - for APA – and 0.6 % - for GPG. This shows an acceptable match between experimental and simulation values. Figure 4.15 shows the sandwich deformation along with the failure zones and FLC, which shows the preliminary stage of failure zone in the sheets. The color coding helps to visualize the different zones – failure, marginal, safe, compression, loose and high wrinkle tendency – which exists in both contour plots and corresponding FLDs.

Along with FLD, dome height till (just before) failure – also known as Limit Dome Height (LDH) – graphs have been extracted from the simulations. From all the simulation conditions, maximum dome height have been recorded at blank #4 for APA (0.015 friction coefficient) and at blank #2 for GPG (0.005 friction coefficient). This indicates that better formability is achieved when friction is decreased to a minimum possible value. This is because the material can easily flow for smaller frictional restrictions. For illustration, graphs for all blank geometry and process parameters are shown in Fig. 4.19 and 4.20.

Another crucial process parameter being studied is the punch velocity, which has a direct correlation with forming speed. Two punch velocities (5000 & 10000 mm/min) have been applied – with considerable gap between the two – to see the effects clearly.

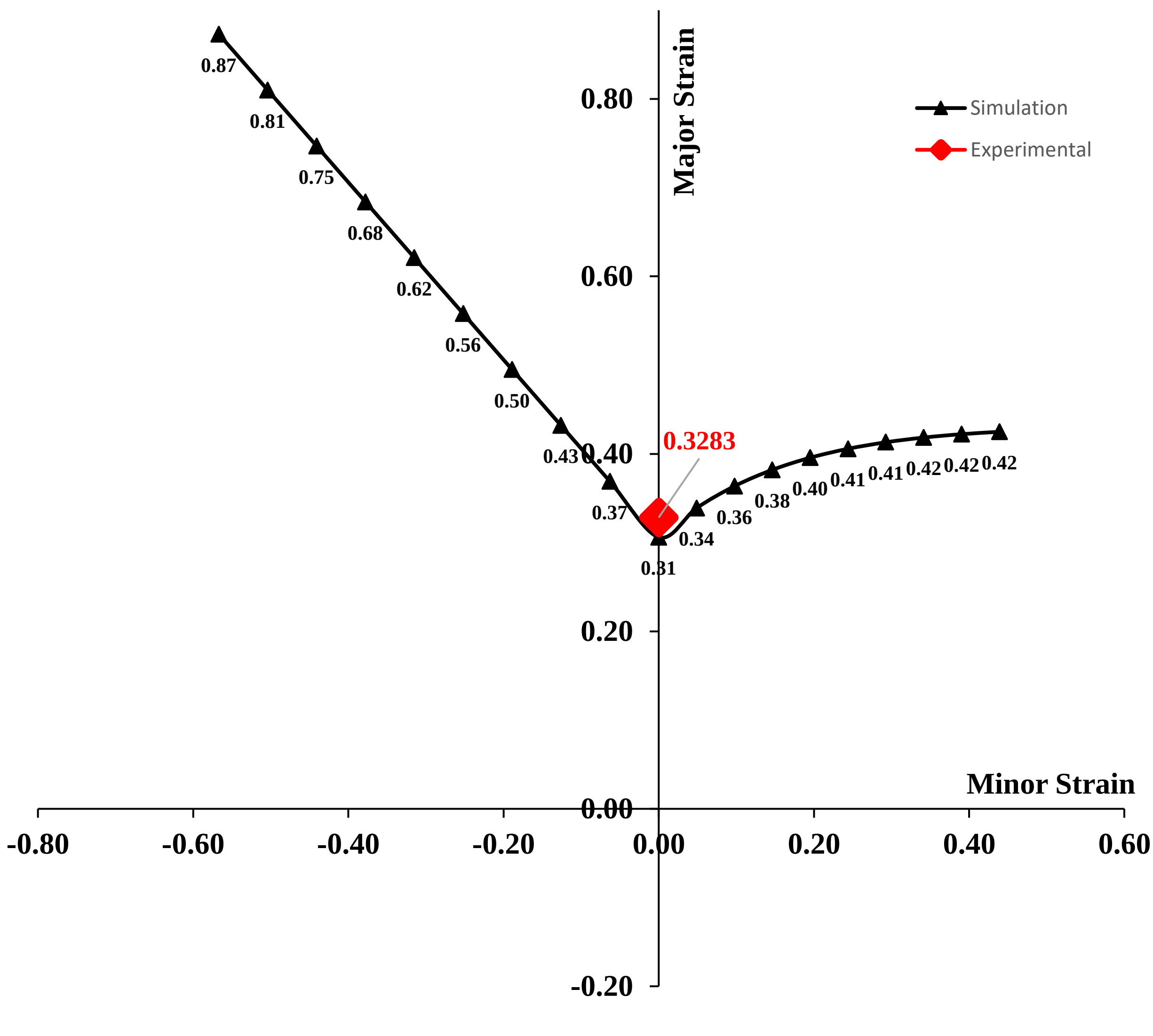

Figure 4. 17: FLC of APA

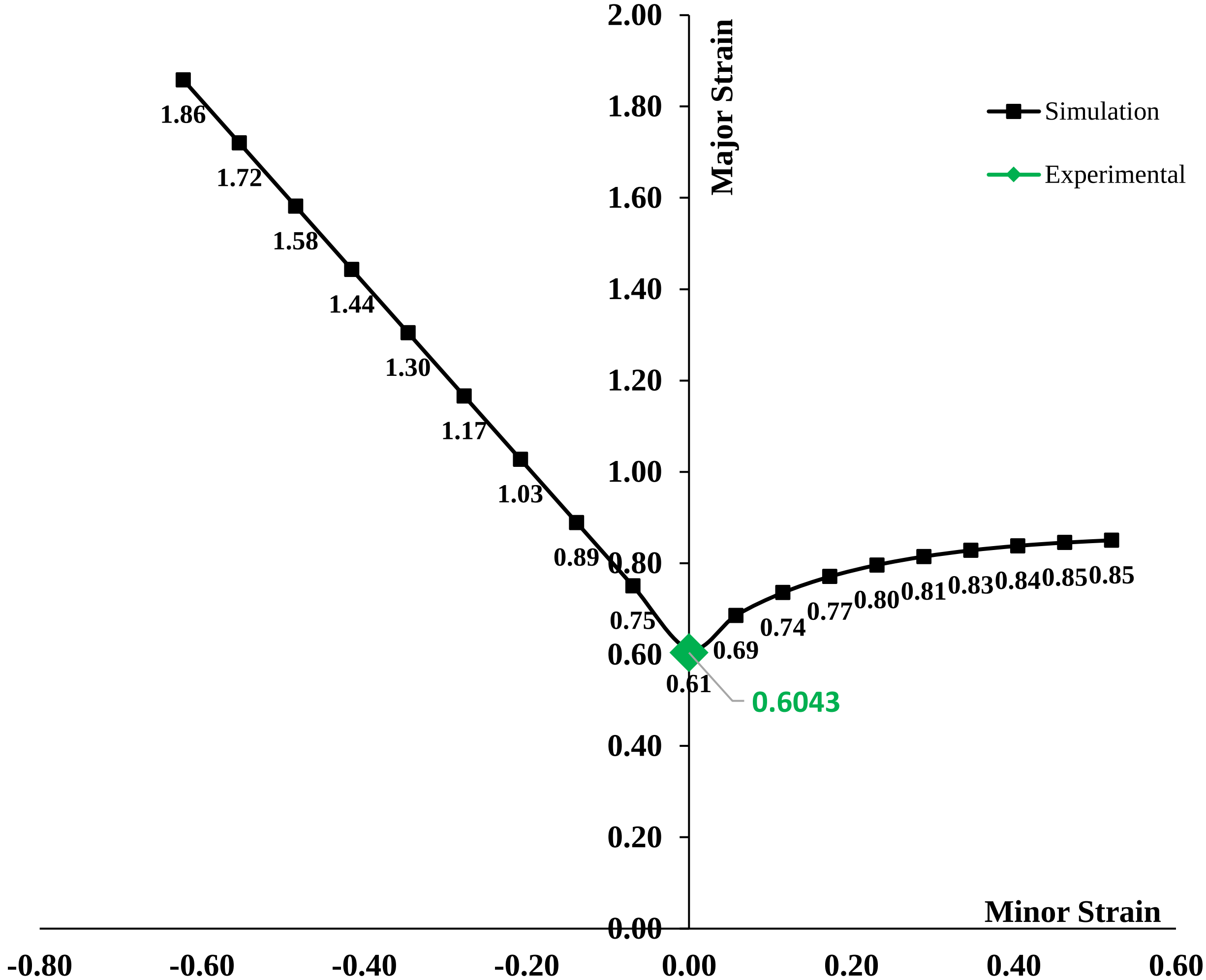

Figure 4. 18: FLC of GPG

Maximum LDH for both APA and GPG is attained with 5000 mm/min punch velocity. For the larger value of punch velocity, however, poor formability is observed, with the blank material being rapidly drawn into failure. As the forming speed is lowered, the material had enough time to flow and take the shape being imposed with the tooling. For instance, blank #8 is formed with 10000 mm/min punch velocity, and it can be observed that small LDH is attained for both blank materials (as shown in Fig. 4.19 and 4.20).

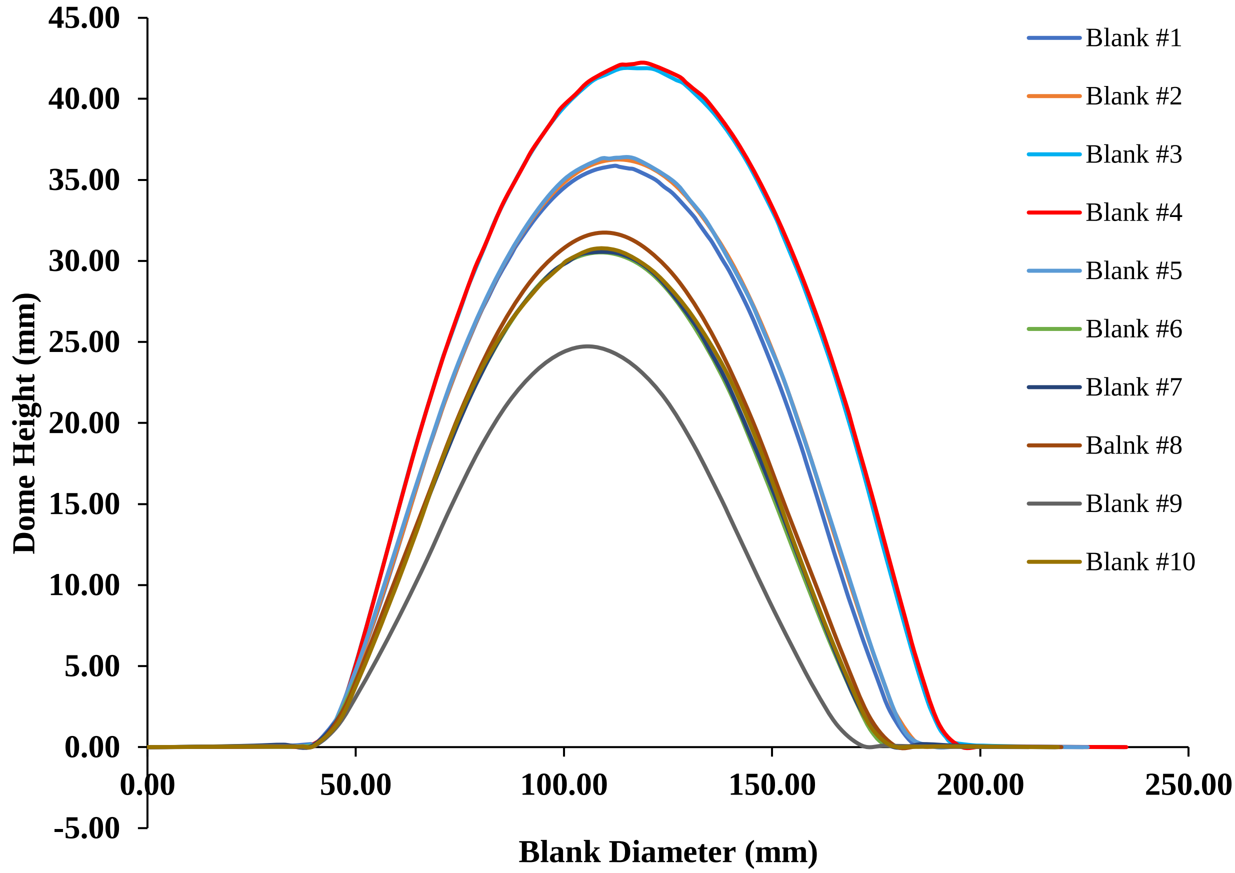

Figure 4. 19: Limiting Dome Height (LDH) of APA

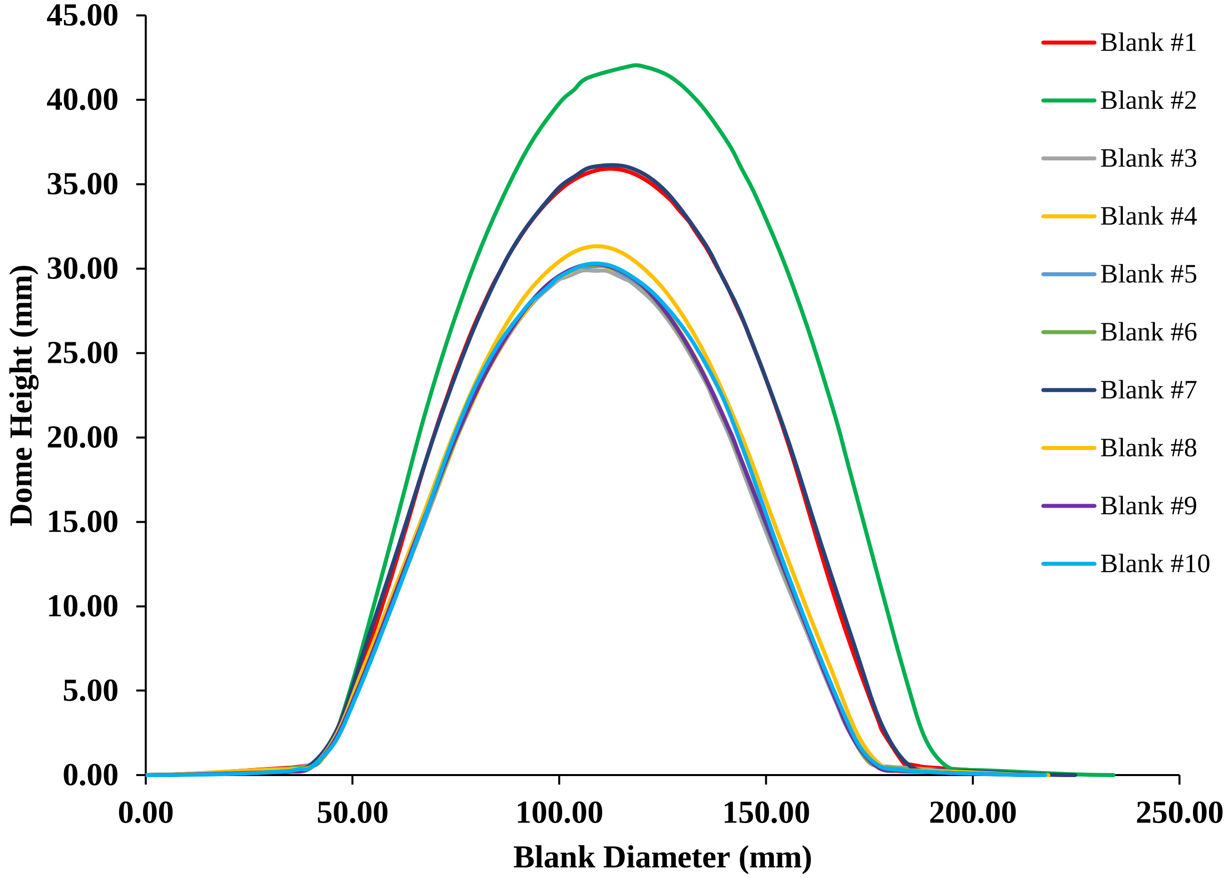

Figure 4. 20: Limiting Dome Height (LDH) of GPG

4.8 Density

For the same volume of rigid materials, their weight variation arises due to their density differences. Using the concept of composite density computation, the densities of MPM sandwich composites have been evaluated and the obtained results are tabularized in Table 4.4 as follows:

Table 4. 4: Density of MPM composites

Material	Density (g/cm^3)
APA	2.436
GPG	5.68882

To get an understanding of how much weight is going to be reduced with the use of MPM sandwich composite instead of mono-lithic metallic sheets, let's consider a 100 cubic centimeter material (for comparison between mono-lithic metallic sheets and MPM sandwich composites) and multiply this volume with the densities in order to find their masses. Table 4.5 illustrates these findings as follows:

Table 4. 5: Masses of 100 cm^3 volume of materials

Material	Density (g/cm^3)	Mass of 100 cm^3 volume (g)
Al	2.7	270
APA	2.436	243.6
GSS	7.874	787.4
GPG	5.68882	568.882

From Table 4.5 the following points can be inferred:

- Using APA instead of Al-sheet, for comparable volume, provides 9.777% weight reduction.
- Using GPG instead of GSS, for comparable volume, provides 27.75% weight reduction.

These are considerable amounts of weight reduction for mass-critical design sectors like automobile, aerospace and marine industries. Hence, application of MPM sandwich composites minimizes fuel consumption and energy requirements of these transportation systems.

CHAPTER 5
Conclusion and Recommendations

5.1 Conclusion

In the present work, MPM sandwich composites' formability was investigated with single strain path experimentations and multiple strain path limit dome height (LDH) simulations, which have been performed using Hyperworks FEA software. The sandwich sheets were made up of aluminum and galvanized steel sheets with PVC – and structural epoxy adhesive as binding agent.

The mechanical properties of base materials – Al-sheet, GSS, PVC and epoxy adhesive – were obtained from uniaxial tension tests, plane-strain tests, plastic-ratio tests and single lap adhesive tests. The MPM sandwich composites – APA and GPG – have also undergone these experimentations. These characteristics were then incorporated into FEA simulations for further analysis.

The hardening exponent (n) of composite laminates and respective metallic constituents were comparable. Hence, their strain hardening phenomena was found to be analogous.

The single-lap adhesive test results revealed that the epoxy adhesive provides sufficient bonding between the metallic sheets and the polymeric core. Even though the PVC sheet ruptured prior to adhesive failure in both cases, the bond between Al-sheet and PVC was stronger than the bond between GSS and PVC since some form of delamination was observed when the GPG composites undergone single strain path tests. This was due to the high abrasion resistance of GSS. In order to achieve better bond strength WRB technique should be applied.

From the density analysis, it has been observed that weight reduction of 9.777 % - for APA – and 27.75 % - for GPG – were achieved compared to Al-sheet and GSS respectively.

The LDH simulations were conducted under two levels of punch velocities (5000 and 10000mm/min), and many levels of frictional conditions – staring from zero. The data extracted from all of the simulations were FLD and maximum dome height. It was observed that the maximum dome height was seen at blank #4 for APA (0.015 friction coefficient) and at blank #2 for GPG (0.005 friction coefficient). In both cases, the punch velocity was 5000 mm/min.

Standard error of 5.6 % - for APA – and 0.6 % - for GPG have been found when comparison of FLC_0 values is made between experiment and simulation. This shows an acceptable match between experimental and simulation values.

It has also been observed that LDH simulations are very sensitive to friction and have influence on the test outputs. Friction at tool-blank interface has considerable effect on formability and thinning distribution. When friction is zero (imaginary and can only be achieved via simulation), the maximum thinning occurs at the tip of the dome. Generally, location of maximum thinning moves away from the apex of the dome (moves toward die corner radius) as interface friction increases, and punch force also increases as interface friction increases. Hence, applying suitable lubricant improves the formability of the sheets.

Better formability – larger dome height – of MPM sandwich composite is associated with small friction coefficient at blank-tool interface and lower forming speed.

5.2 Recommendation

In manufacturing, it is common to specify and select suitable and reliable materials that can fulfill product's requirements. Sometimes, already existing materials are able to accomplish these demands with or without necessary modifications. Otherwise, new materials are designed and manufactured according to necessities of the product being manufactured.

Afterall, materials are innovated, researched, enhanced and manufactured for usage in some product. These MPM sandwich composites are also intended to be utilized in various industries especially when weight reduction is needed.

MPM sandwiched composite plates (primarily, aluminum panels) have been extensively utilized in construction sector. These panels are used for finishing houses and interior design, partition creation, outer building decoration, construction of studios (because of its sound deadening capability) etc. Almost all of the aforementioned applications, however, do not require the aluminum panel to be formed into complex geometries, only flat shaped ones trimmed into required dimensions are applied.

As it has been studied in this thesis, however, MPM sandwich composites are not restricted to aluminum panel plates. A variety of sheet metals (like steel, aluminum and their alloys, etc.) can be laminated with different polymer plastics (like PVC, PU, PE, PP, etc.) to provide various MPM laminate composites.

These composites can have a wide range of application in aerospace, marine and automobile industries (especially, due to their substantial strength to weight ratio). Among the aforementioned industries, this work focused on automobile industry as an application area since more and more car assembly factories are being installed in our country nowadays. Some sub-components can be manufactured here in accordance with design specifications of the automobile company with MPM sandwiched composites. Their thickness, weight, strength and formability can be adjusted by careful selection of substrate materials (sheet metal, polymeric core and adhesive) with the required thickness and performance.

These MPM laminated composites can be used for the hood (bonnet) and the roof of an automobile as shown in the Fig. 5.1 [green] of a typical automobile below. These two parts of an automobile are ideal for weight reduction since they cover large portion of the car, which account for approximately 8 percent of the total automobile weight (Nicholas Lutsey, 2010). In addition, thermal insulation characteristics of the MPM composite helps in reduction of heat that could be conducted from sun and would have raised the car's interior temperature. This insulation occurs because of the polymeric core sandwiched between the metallic sheets. Another advantage of these composites is their sound proofing (deadening) behavior (again attributable to the polymeric core embedded in between the metallic sheets). As a result, noises coming from rain drops and vibration of moving parts in the car can be dampened considerably.

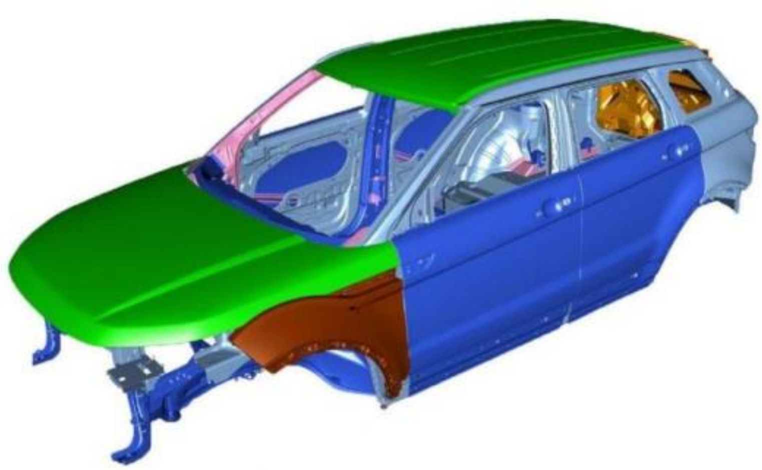

Figure 5. 1: Range Rover Evoque (Source: Land Rover)

Hydroforming techniques are recommended to make the previously mentioned automobile components with MPM sandwiched composites. The reason behind is that, hydroforming is a specialized type of die forming that uses a high-pressure hydraulic fluid to press room temperature working material into a die which is capable of formation of complex shaped parts with a higher stiffness-to-weight ratio and at a lower per unit cost than traditional stamped parts (M. Zampaloni *et al.*, 2003). Furthermore, hydroforming allows the sheet to deform uniformly (uniform distribution of strains) resulting in reduced thinning in the final part.

Since these MPM sandwiched composites can be drilled, mechanical fasteners (like screws, bolts and nuts) can be used to assemble parts made from these materials with other body parts of the automobile. Moreover, industrial structural adhesives play a vital role in assembly of composites.

5.3 Future research areas

This study examined the formability of two types of MPM sandwich composites. The investigation focuses on how much deformation can these laminates withstand before excessive thinning and failure. However, their spring back phenomena is not studied in the present work and it should be a subject of study for future research.

Moreover, since these composites are comprised of heterogeneous materials, their thermal conductivity is somewhat complex. Hence, thermal analysis of various MPM laminates should be incorporated in future researches.

References

Aghchai, A. J., & Khatami, S. (2018). Experimental and numerical formability investigation of FML sheets with glass fiber reinforced core. The International Journal of Advanced Manufacturing Technology, 96(9-12), 3881-3891.

Alipour, M., Torabi, M. A., Sareban, M., Lashini, H., Sadeghi, E., Fazaeli, A., & Hashemi, R. (2020). Finite element and experimental method for analyzing the effects of martensite morphologies on the formability of DP steels. Mechanics Based Design of Structures and Machines, 48(5), 525-541.

Atul S, T., & Babu, M. L. (2019). A review on effect of thinning, wrinkling and spring-back on deep drawing process. Proceedings of the Institution of Mechanical Engineers, Part B: Journal of Engineering Manufacture, 233(4), 1011-1036.

Baldan, A. (2004). Adhesively-bonded joints in metallic alloys, polymers and composite materials: Mechanical and environmental durability performance. Journal of Materials Science, 39(15), 4729-4797.

Burchitz, I., Boesenkool, R., van der Zwaag, S., & Tassoul, M. (2005). Highlights of designing with Hylite–a new material concept. Materials & design, 26(4), 271-279.

Carradò, A., Faerber, J., Niemeyer, S., Ziegmann, G., & Palkowski, H. (2011). Metal/polymer/metal hybrid systems: Towards potential formability applications. Composite Structures, 93(2), 715-721.

Carradò, A., Sokolova, O., Ziegmann, G., & Palkowski, H. (2010). Press joining rolling process for hybrid systems. In Key Engineering Materials (Vol. 425, pp. 271-281). Trans Tech Publications Ltd.

Chen, F. K., & Lin, S. Y. (2007). A formability index for the deep drawing of stainless steel rectangular cups. The International Journal of Advanced Manufacturing Technology, 34(9-10), 878.

Chen, C., Li, B., Kanari, M., & Lu, D. (2019). Epoxy Adhesives. In Adhesives and Adhesive Joints in Industry Applications. IntechOpen.

Clearfield, H. M., McNamara, D. K., & Davis, G. D. (1991). Adherend surface preparation for structural adhesive bonding. In Adhesive bonding (pp. 203-237). Springer, Boston, MA.

Cochis, A., Rimondini, L., Pourroy, G., Stanic, V., Palkowski, H., & Carradò, A. (2013). Biomimetic calcium–phosphates produced by an auto-catalytic route on stainless steel 316L and bio-inert polyolefin. RSC advances, 3(28), 11255-11262.

Dhaiban, A. A., Soliman, M. E. S., & El-Sebaie, M. G. (2014). Finite element modeling and experimental results of brass elliptic cups using a new deep drawing process through conical dies. Journal of Materials Processing Technology, 214(4), 828-838.

DiCello, J. A. (1980). Steel-polypropylene-steel laminate—a new weight reduction material. SAE Transactions, 491-505.

Engel, B., & Buhl, J. (2011). Metal forming of vibration-damping composite sheets. Steel research international, 82(6), 626-631.

Esther, r-value and related parameters, Bailey Metal Processing, southern Ontario, Canada (2017).

Friction Factors - Coefficients of Friction. Archived from the original. URL: https://web.archive.org/web/20190201171526/http:/www.roymech.co.uk/Useful_Tables/Tribology/co_of_frict.htm#method

Ghazanfari, A., Soleimani, S. S., Keshavarzzadeh, M., Habibi, M., Assempuor, A., & Hashemi, R. (2020). Prediction of FLD for sheet metal by considering through-thickness shear stresses. Mechanics Based Design of Structures and Machines, 48(6), 755-772.

Gholamzadeh Babaki, M. H., & Shakouri, M. (2019). Free and forced vibration of sandwich plates with electrorheological core and functionally graded face layers. Mechanics Based Design of Structures and Machines, 1-18.

Gorji, A., Alavi-Hashemi, H., Bakhshi-Jooybari, M., Nourouzi, S., & Hosseinipour, S. J. (2011). Investigation of hydrodynamic deep drawing for conical–cylindrical cups. The International Journal of Advanced Manufacturing Technology, 56(9), 915-927.

Ghosh, A. K., & Hecker, S. S. (1975). Failure in thin sheets stretched over rigid punches. Metallurgical Transactions A, 6(5), 1065-1074.

Guide to Bonding, by Plexus Structural Adhesives. *URL: https://www.curbellplastics.com/Research Solutions/Technical-Resources/Technical-Resources/Plexus-Adhesives-Guide-to-Bonding*

Harhash, M., Carrado, A., & Palkowski, H. (2014). Forming limit diagram of steel/polymer/steel sandwich systems for the automotive industry. In Advanced composites for aerospace, marine, and land applications (pp. 243-254). Springer, Cham.

Harhash, M., Palkowski, H., & Carradò, A. (2015). Forming potential of low-density laminates. In Niedersächsisches Symposium Materialtechnik (pp. 53-60).

Harhash, M., Gilbert, R. R., Hartmann, S., & Palkowski, H. (2020). Experimental characterization, analytical and numerical investigations of metal/polymer/metal sandwich composites–Part 2: Free bending. Composite Structures, 232, 111421.

Harhash, M., Gilbert, R. R., Hartmann, S., & Palkowski, H. (2018). Experimental characterization, analytical and numerical investigations of metal/polymer/metal sandwich composites–Part 1: Deep drawing. Composite structures, 202, 1308-1321.

Harhash, M., Sokolova, O., Carradó, A., & Palkowski, H. (2014). Mechanical properties and forming behaviour of laminated steel/polymer sandwich systems with local inlays–Part 1. Composite Structures, 118, 112-120.

Johnson, W. S. (1988). Adhesively bonded joints: testing, analysis, and design (Vol. 981). ASTM International.

Kami, A., Dariani, B. M., Comsa, D. S., Banabic, D., Vanini, A. S., & Liewald, M. (2017, July). An experimental study on the formability of a vibration damping sandwich sheet (BONDAL). In Proc Rom Acad Ser A (Vol. 18, No. 3, pp. 281-290).

Kami, A., Dariani, B. M., Comsa, D. S., Vanini, A. S., & Liewald, M. (2016). Calibration of GTN damage model parameters using hydraulic bulge test. The Romanian Journal of Technical Sciences. Applied Mechanics., 61(3), 245-260.

Karlsson, K. F., & TomasÅström, B. (1997). Manufacturing and applications of structural sandwich components. Composites Part A: Applied Science and Manufacturing, 28(2), 97-111.

Keeler, S. P. (1978). Forming limit criteria—sheets. In Advances in deformation processing (pp. 127-157). Springer, Boston, MA.

Keipour, S., & Gerdooei, M. (2019). Springback behavior of fiber metal laminates in hat shaped draw bending process: experimental and numerical evaluation. The International Journal of Advanced Manufacturing Technology, 100(5), 1755-1765.

Kim, K. J., Rhee, M. H., Choi, B. I., Kim, C. W., Sung, C. W., Han, C. P., ... & Won, S. T. (2009). Development of application technique of aluminum sandwich sheets for automotive hood. International Journal of Precision Engineering and Manufacturing, 10(4), 71-75.

Kim, J. K., & Yu, T. X. (1997). Forming and failure behaviour of coated, laminated and sandwiched sheet metals: a review. Journal of Materials Processing Technology, 63(1-3), 33-42.

Kim, K. J., Kim, D., Choi, S. H., Chung, K., Shin, K. S., Barlat, F., ... & Youn, J. R. (2003). Formability of AA5182/polypropylene/AA5182 sandwich sheets. Journal of Materials Processing Technology, 139(1-3), 1-7.

Kim, J. K., & Yu, T. X. (1997). Forming and failure behaviour of coated, laminated and sandwiched sheet metals: a review. Journal of Materials Processing Technology, 63(1-3), 33-42.

Kim, D., Kim, H., Kim, J. H., Lee, M. G., Kim, K. J., Barlat, F. & Chung, K. (2015). Modeling of forming limit for multilayer sheets based on strain-rate potentials. International Journal of Plasticity, 75, 63-99.

Kim, K. J., Kim, D., Choi, S. H., Chung, K., Shin, K. S., Barlat, F., ... & Youn, J. R. (2003). Formability of AA5182/polypropylene/AA5182 sandwich sheets. Journal of Materials Processing Technology, 139(1-3), 1-7.

Kim, K. J., Kim, C. W., Choi, B. I., Sung, C. W., Kim, H. Y., Won, S. T., & Ryu, H. Y. (2008). Formability of aluminum 5182-polypropylene sandwich sheet for automotive application. Journal of Solid Mechanics and Materials Engineering, 2(4), 574-581.

Kilfoil, L. J. (2007). In-plane plane strain testing to evaluate formability of sheet steels used in tubular products. Kingston: Queen's University.

Levy, B. S., & Van Tyne, C. J. (2016). An approach to predicting the forming limit stress components from mechanical properties. Journal of Materials Processing Technology, 229, 758-768.

Link, T. M. (2001). Formability and performance of steel-plastic-steel laminated sheet materials. SAE transactions, 48-55.

Liu, Y., & Glass, G. (2013). Effects of mesh density on finite element analysis (No. 2013-01 1375). SAE Technical Paper.

Lutsey, N. (2010). Review of technical literature and trends related to automobile mass reduction technology.

Magalhães, A. G., De Moura, M. F. S. F., & Gonçalves, J. P. M. (2005). Evaluation of stress concentration effects in single-lap bonded joints of laminate composite materials. International journal of adhesion and adhesives, 25(4), 313-319.

Makinouchi, A., Ogawa, H., & Hashimoto, K. (1987). Finite element simulation of bending process of steel-plastic laminate sheets. In Studies in Applied Mechanics (Vol. 15, pp. 221-230). Elsevier.

Makinouchi A, Yoshida S, Ogawa H. Finite element simulation of bending process of steel plastic laminate sheets. J JSTP 1988; 29:755–60.

Materials Thermal Properties Database, *URL: https://thermtest.com/thermal-resources/materials database#:~:text=Thermal%20properties%20include%20thermal%20conductivity,thermal%20effusivity%2C%20and%20material%20density.*

Mousa, S., & Kim, G. Y. (2017). A direct adhesion of metal-polymer-metal sandwich composites by warm roll bonding. Journal of Materials Processing Technology, 239, 133-139.

Mousa, S., & Kim, G. Y. (2015, June). Direct adhesion of warm roll-bonded al1100/polyurethane/al1100 sandwich composite. In International Manufacturing Science and Engineering Conference (Vol. 56826, p. V001T02A101). American Society of Mechanical Engineers.

Mousa, S., & Kim, G. Y. (2015). Experimental study on warm roll bonding of metal/polymer/metal multilayer composites. Journal of Materials Processing Technology, 222, 84-90.

Padmanabhan, R., Oliveira, M. C., Alves, J. L., & Menezes, L. F. (2007). Influence of process parameters on the deep drawing of stainless steel. Finite Elements in Analysis and Design, 43(14), 1062-1067.

Palkowski, H., & Carrado, A. (2014). Three-layered sandwich material for lightweight applications. Emerging Materials Research, 3(3), 130-135.

Paul, S. K. (2021). Controlling factors of forming limit curve: A review. Advances in Industrial and Manufacturing Engineering, 100033.

Raghavan, K. S. (1995). A simple technique to generate in-plane forming limit curves and selected applications. Metallurgical and materials transactions A, 26(8), 2075-2084.

Reitz, W. E., & Oman, R. M. (2000). How to join plastics. Advanced materials & processes, 158(3), 49-49.

Rotheiser, J. (2015). Joining of plastics: handbook for designers and engineers. Carl Hanser Verlag GmbH Co KG.

Ruokolainen, R. B., & Sigler, D. R. (2008). The effect of adhesion and tensile properties on the formability of laminated steels. Journal of Materials Engineering and Performance, 17(3), 330-339.

Safaei, B., Moradi-Dastjerdi, R., Behdinan, K., Qin, Z., & Chu, F. (2019). Thermoelastic behavior of sandwich plates with porous polymeric core and CNT clusters/polymer nanocomposite layers. Composite Structures, 226, 111209.

Shaffer DK, Clearfield HM, Ahearn JS. In: Minford JD, editor. Treatise on adhesion and adhesives, vol. 7. New York: Marcel Dekker, 1991.

Sokolova, O., Carradó, A., & Palkowski, H. (2010). Production of customized high-strength hybrid sandwich structures. In Advanced materials research (Vol. 137, pp. 81-128). Trans Tech Publications Ltd.

Sokolova, O. A., Carradò, A., & Palkowski, H. (2011). Metal–polymer–metal sandwiches with local metal reinforcements: A study on formability by deep drawing and bending. Composite Structures, 94(1), 1-7.

Sokolova, O. A., Kühn, M., & Palkowski, H. (2012). Deep drawing properties of lightweight steel/polymer/steel sandwich composites. Archives of Civil and Mechanical Engineering, 12(2), 105-112.

Somayajulu, T. S. (2004). Vibration and formability characteristics of aluminum-polymer sandwich materials (Doctoral dissertation, University of Michigan College of Engineering Graduate Professional Programs).

Takalkar, A., Rao, J. M. K., & Babu, L. M. C. (2015). Numerical simulation for predicting failure in deep drawing process using forming limit diagram (FLD). Int J Adv Mech Civ Eng, 2(4), 11-15.

THYSSENKRUPP STEEL, A. (2012). Litecor: the intelligent solution for cost-effective lightweight design. Germany: Duisburg.

Veenstra, E. W. (1993). Aluminum-plastic-aluminum sandwich sheet for maximum weight reduction in body panels (No. 930706). SAE Technical Paper.

Wegman, R. F., & Van Twisk, J. (2012). Surface preparation techniques for adhesive bonding.

Wollmann, T., Hahn, M., Wiedemann, S., Zeiser, A., Jaschinski, J., Modler, N., ... & Paul, C. (2018). Thermoplastic fibre metal laminates: Stiffness properties and forming behaviour by means of deep drawing. Archives of Civil and Mechanical Engineering, 18(2), 442-450.

Yao, H., Chen, C. C., Liu, S. D., Li, K. P., Du, C., & Zhang, L. (2003). Laminated steel forming modeling techniques and experimental verifications (No. 2003-01-0689). SAE Technical Paper.

Yazdi, M. S., Bakhshi-Jooybari, M., Gorji, H., Shakeri, M., & Khademi, M. (2018). Investigation of forming cylindrical parts in a modified hydrodynamic deep drawing assisted by radial pressure with inward flowing liquid. Journal of Manufacturing Science and Engineering, 140(3).

Yoon, J. Y. (2012). Evaluation of formability and determination of flow stress curve of sheet materials with dome test (Doctoral dissertation, The Ohio State University).

Zampaloni, M., Abedrabbo, N., & Pourboghrat, F. (2003). Experimental and numerical study of stamp hydroforming of sheet metals. International Journal of Mechanical Sciences, 45(11), 1815-1848.

Appendix

A. LDH of APA – Blank #1 & #10

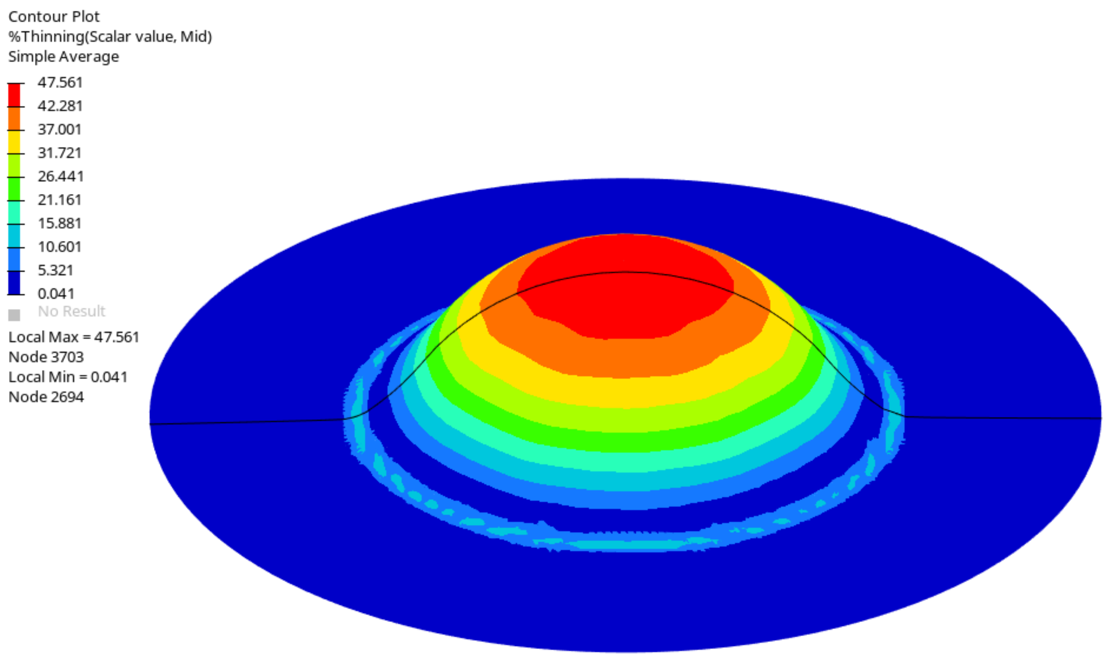

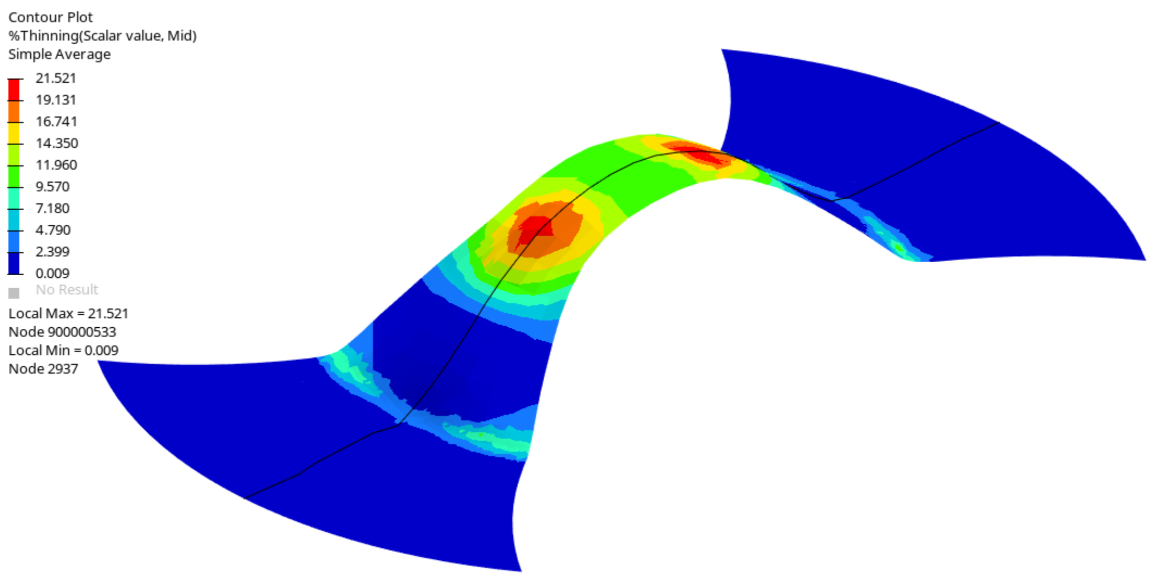

B. LDH of GPG – Blank #1 & #10